



Selective Cu(I) complex with phosphine-peptide (**SarGly**) conjugate contra breast cancer: Synthesis, spectroscopic characterization and insight into cytotoxic action

Urszula K. Komarnicka^{a,*}, Sandra Kozieł^a, Radosław Starosta^a, Agnieszka Kyzioł^b

^a Faculty of Chemistry, University of Wrocław, Joliot-Curie 14, 50-383 Wrocław, Poland

^b Faculty of Chemistry, Jagiellonian University, Gronostajowa 2, 30-387 Kraków, Poland

ARTICLE INFO

Keywords:

Peptide carriers
Copper(I) complex
Conjugate
DNA
ROS
Breast cancer

ABSTRACT

The main disadvantage of conventional anticancer chemotherapy is the inability to deliver the correct amount of drug directly to cancer. Those molecular delivering systems are very important to destroy cancer cells selectively. Herein we report synthesis of phosphine-peptide conjugate (Ph₂PCH₂-Sar-Gly-OH, **PSG**) derived from **SarGly** (sarcosine-glycine), which can be easily exchanged to other peptide carriers, its oxide (OPh₂PCH₂-Sar-Gly-OH, **OPSG**) and the first copper(I) complex ([Cu(dmp)(P(Ph)₂CH₂-Sar-Gly-OH)]), **1-PSG**, where dmp stands for 2,9-dimethyl-1,10-phenanthroline). The compounds were characterized by elemental analysis, NMR (1D, 2D), UV-Vis spectroscopy and DFT (Density Functional Theory) methods. **PSG** and **1-PSG** proved to be stable in biological medium in the presence of atmospheric oxygen for several days. The cytotoxicity of the compounds and cisplatin was tested against cancer cell lines: mouse colon carcinoma (CT26; ^{1-PSG}IC₅₀ = 3.12 ± 0.1), human lung adenocarcinoma (A549; ^{1-PSG}IC₅₀ = 2.01 ± 0.2) and human breast adenocarcinoma (MCF7; ^{1-PSG}IC₅₀ = 0.98 ± 0.2) as well as against primary line of human pulmonary fibroblasts (MRC-5; ^{1-PSG}IC₅₀ = 78.56 ± 1.1). Therapeutic index for **1-PSG** (MCF7) equals 80. Intracellular accumulation of **1-PSG** complex increased with time and was much higher (96%) inside MCF7 cancer cells than in normal MRC5 cells (20%). Attachment of **SarGly** to cytotoxic copper(I) complex *via* phosphine motif improved selectivity of copper (I) complex **1-PSG** into the cancer cells. Precise mechanistic study revealed that the **1-PSG** complex causes apoptotic cells MCF7 death with simultaneous decrease of mitochondrial membrane potential and increase of caspase-9 and -3 activities. Additionally, **1-PSG** generated high level of reactive oxygen species that was the reason for oxidative damages to the sugar-phosphate backbone of plasmid DNA.

1. Introduction

Mortality caused by cancer is about to exceed that from cardiovascular diseases in near future. Approximately 7 million people die from cancer-related cases per year, and it is estimated that there will be > 16 million new cancer cases every year by 2020 [1,2]. Chemotherapy is still one of the major approaches to treat cancer by delivery of a cytotoxic agent to cancer cells. However, the main disadvantage of conventional chemotherapy is the inability to deliver the correct amount of drug directly to cancer cells without affecting healthy cells [3]. Drug resistance, altered biodistribution, biotransformation, and drug clearance are also considered common problems [3]. This shows the importance of development of systems that will selectively destroys cancer cells [4–7].

Various opportunities for the design of therapeutic agents can be

offered by medicinal inorganic chemistry (very often not accessible to organic compounds). Coordinated chemistry of metal-based drugs has been placed in the frontline in the fight against cancer by widespread use of cisplatin. Unfortunately, the use of this drug is very limited due to its high toxicity [8]. Copper-based complexes could be less toxic for normal cells with respect to cancer cells, despite copper toxicity related to its redox activity. Also, a different response of normal and tumor cells to copper ions can be a platform for development of copper complexes endowed with antineoplastic characteristic [8–10].

Copper(I) complexes constitute a group of compounds that is still not exploited enough, but over the last several years, we can observe a significant interest increase of their anticancer [11–17], antibacterial [18], antiviral [19,20], antifungal [21], and inflammatory [14] activity. Furthermore, the phosphine ligands forms a strong bond with copper(I) ion which prevents oxidation of the phosphine ligand and

* Corresponding author.

E-mail address: urszula.komarnicka@chem.uni.wroc.pl (U.K. Komarnicka).

copper(I) to copper(II) [12], what was also proven in our previous studies [13–17,22–24]. Additionally, phosphine ligands can be easily functionalized, which is remarkable. In particular, aminomethylphosphanes derived from amino acids [25–28] or prepared from the highly water-soluble aliphatic secondary amines [29,30], seem to be interesting in terms of the formation of potential conjugates with a wide range of biomolecules. This makes them good candidates for drugs.

Linking of the peptides (described as a carriers) via phosphine motif to copper(I) complexes [13,22–24,31–34], may enable selective delivery of these coordination compounds to the tumor cells. Examples of such peptides carriers are RGD (Arg-Gly-Asp) motif and other NGR peptide (Asn-Gly-Arg) selectively recognize integrins - proteins responsible for the growth, division, adhesion and migration of cancer cells (peptides that have entered clinical trials). It is worth noting that mentioned motifs combined with doxorubicin, paclitaxel and fluorouracil cause significant decrease of *in vivo* toxicity of these drugs [35–40]. In this paper we propose a novel approach – connecting peptides, in our case: sarcosine-glycine (SarGly) with copper(I) complexes. We decided to choose this peptide SarGly, because of several reasons. Firstly, SarGly is small and cheap molecule and we could establish synthetic conditions before applying it to our research peptides as RGD or NRG (very expensive). Initial, presented here, results were surprisingly good, so we decided to continue research with this compound SarGly. Secondly, motif GlySar was reported as a PET tracer targeted to the PEPTs (H⁺/peptide transporters – functionally expressed in some human cancer cell lines) for cancer detection in mice [41,42]. It is worth mentioning that peptides possess well-known advantages as drugs, such as specificity, potency, and low toxicity [43]. To the best of knowledge, in the literature there are no such systems reported so far.

This article is continuation of our previous projects describing copper(I) complexes bearing phosphine ligands derived from fluoroquinolone antibiotics [14–17,50,51,58,65]. We demonstrated high cytotoxic activity towards view cancer lines of inorganic derivatives of fluoroquinolones. It was proven that mentioned above compounds caused apoptotic cancer cell death via caspase-dependent mitochondrial pathway. Unfortunately, we were struggling with high toxicity of those complexes. That is why we decided to exchange fluoroquinolone molecule to some simple, cheap and lipophilic peptides.

In this paper we describe synthesis of phosphine ligand (PPh₂CH₂-Sar-Gly-OH; PSG) derived from sarcosine-glycine (SarGly), its oxide (OPPh₂CH₂-Sar-Gly-OH; OPSG) and copper(I) complex [CuI(2,9-dimethyl-1,10-phenanthroline)PSG] (1-PSG). Physicochemical properties of all these compounds were detected using elemental analysis, NMR (1D and 2D), UV-Vis spectroscopy and theoretical calculations. Cytotoxic activity *in vitro* of SarGly and its organic (PSG, OPSG) and inorganic (1-PSG) derivatives was tested against three cancer cell lines: mouse colon carcinoma (CT26), human lung adenocarcinoma (A549) and human breast adenocarcinoma (MCF7) as well as one primary line of human pulmonary fibroblasts (MRC5). Herein, we also try to approach the mechanism of 1-PSG cytotoxic action towards human breast adenocarcinoma (MCF7). To realize our goal we undertook a series of experiments: (i) intracellular uptake of the tested complex was studied by ICP-MS spectrometry; (ii) the mode of cell death was examined by flow cytometric analysis; (iii) level of mitochondrial membrane potential was measured; (iv) activity of caspases 3 and 9 was determined; (v) the ability of the complexes to generate reactive oxygen species (ROS) in the cells was examined using two different fluorescent probes; (vi) generation of oxidative DNA cleavage was studied by gel electrophoresis.

2. Experimental part

2.1. Materials

All reactions were carried out under a dinitrogen atmosphere using

standard Schlenk techniques. PPh₂(CH₂OH)₂Cl was synthesized according to a literature procedures [44]. Peptide SarGly was purchased from Bachem (Switzerland). Ph₂PH, dmp, CuI, other small chemicals and solvents were purchased from Sigma-Aldrich (Germany) and used without further purifications. All solvents were deaerated before use.

2.2. Methods

Elemental analyses were performed on a Vario EL3 CHN analyser for C, H, and N, and they were within 0.3% of the theoretical values. NMR spectra were recorded on a Bruker AMX 500 spectrometer (at 298 K) with traces of solvent as an internal reference for ¹H (DMSO-*d*₆: 2.50 ppm) and ¹³C spectra (DMSO-*d*₆: 39.51 ppm) and 85% H₃PO₄ in H₂O as an external standard for ³¹P. The signals in the spectra are defined as: s = singlet (* – strongly broadened signal), d = doublet, dd – doublet of doublets, t = triplet and m = multiplet. Chemical shifts are reported in ppm and coupling constants are reported in Hz. Absorption spectra were recorded on a Cary 50 Bio spectrophotometer (Varian Inc., Palo Alto, CA) in the 800–200 nm range.

2.3. Synthesis

2.3.1. Preparation of Ph₂P-CH₂-Sar-Gly-OH (PSG)

PPh₂(CH₂OH)₂Cl (0.6434 g, 2.27 mmol) was dissolved in 20 mL of methanol and cooled down using water bath (T = 8 °C). Then, a slight excess of NEt₃ (triethylamine; 2.60 mmol) was added. Mixture was stirred and with time reached room temperature (RT). After 40 min SarGly (0.3320 g, 2.27 mmol) in water (10 mL) was added dropwise into the mixture (RT). After 1 h of stirring, clear solution was observed. Mixture was dried under reduced pressure for few hours. White, crude product was dissolved in water (30 mL; milky solution was observed) and extracted four times with CHCl₃ (10 mL) using cannula. Chloroform phase was dried under pressure and white solid of PSG was formed. It is well soluble in CHCl₃, DMSO, CH₂Cl₂, CH₃CN, moderately in ethanol, methanol and water.

Yield: 90%, **Molar mass:** 344.35 g/mol. **Anal. Calcd** for PC18H21N2O3: C, 62.78; H, 6.15; N, 8.14%. **Found:** C, 62.77; H, 6.16; N, 8.13%.

NMR (DMSO-*d*₆, 298 K): ³¹P{¹H}: -27.08 s, ¹H: H^{Ph}: 7.34–7.55; H^{NH}: 4.41 s; H¹: 3.07 s; H²: 2.31 s; H³: 3.30 d (J = 3.05); H⁵: 3.51 d (J = 5.53); ¹³C{¹H}: C^{Ph(i)}: 137.65 d (J = 12.72); C^{Ph(o)}: 132.72 d (J = 19.07); C^{Ph(m)}: 128.62 d (J = 6.36); C^{Ph(p)}: 128.76 s; C¹: 61.86 d (J = 9.10); C²: 44.29 d (J = 10.0); C³: 60.03 d (J = 4.50); C⁴: 169.37 s; C⁵: 41.99 s; C⁶: 171.62 s.

2.3.2. Preparation of Ph₂P(O)CH₂SG (OPSG)

The oxide derivative was prepared in the reaction of PSG (0.4258 g; 1.24 mmol) dissolved in chloroform (20 mL) with equimolar amount of H₂O₂ (35% solution in water). After 1 h of stirring (RT) the solution was evaporated to dryness. White solid well soluble in CHCl₃, DMSO, CH₂Cl₂, CH₃CN, moderately in ethanol, methanol and water was obtained.

Yield: 100%, **Molar mass:** 360.34 g/mol **Anal. Calcd** for PC18H21N2O4: C, 60.00; H, 5.87; N, 7.77%. **Found:** C, 59.99; H, 5.88; N, 7.76%.

NMR (DMSO-*d*₆, 298 K): ³¹P{¹H}: 26.94 s ¹H: H^{Ph}: 7.76–7.42; H¹: 3.14 s; H²: 2.31 s; H³: 3.52 d (J = 5.34); H⁵: 3.56 d (J = 5.91); ¹³C{¹H}: C^{Ph(o)}: 132.82 d (J = 94.46); C^{Ph(o)}: 131.68 d (J = 1.82); C^{Ph(m)}: 130.74 d (J = 9.08); C^{Ph(p)}: 131.03 d (J = 8.08) s; C¹: 59.89 d (J = 87.19); C²: 44.68 d (J = 6.36); C³: 55.88 d (84.47); C⁴: 169.57 s; C⁵: 40.77 s; C⁶: 171.22 s.

2.3.3. Preparation of the complex with phosphine-peptide conjugate (1-PSG)

Neocuproine (0.1540 g; 0.7396 mmol) and copper iodide (0.1409 g; 0.7396 mmol) were added in equimolar ratios to the phosphine

PPh₂CH₂SG (0.2547 g; 0.7396 mmol) dissolved in 20 mL of chloroform and acetonitrile mixture (V:V = 1:1). After few minutes a cloudy solution was formed, which after half an hour became clear. The light orange precipitate was formed after 24 h of stirring. The solid was filtered off, washed a few times with mixture of water and methanol (v:v = 1:1), and dried under vacuum. The **1-PSG** complex is well soluble in CHCl₃, DMSO and CH₂Cl₂, moderately in CH₃CN, poorly in ethanol and methanol and water.

Yield: 75%, **Molar mass:** 743.05 g/mol **Anal. Calcd** for CuIPC32H33N4O3: C, 51.72; H, 4.48; N, 7.54%. Found: C, 51.71; H, 4.50; N, 7.53%.

NMR (DMSO-*d*₆, 298 K): ³¹P{¹H}: -16.10 s ¹H: H^{Ph}: 7.59–7.24; H¹: 2.96 s; H²: 2.15 s; H³: 3.55 s, H⁵: 3.50 d (J = 5.70); dmpH^{3,8}: 7.78 d (J = 8.20); dmpH^{4,7}: 8.58 d (J = 8.20); dmpH^{5,6}: 8.06 s; dmpH^{15,16}: 2.70 s; ¹³C{¹H}: C^{Ph(O)}: 137.20 s; C^{Ph(O)}: 132.50 d (J = 12.70); C^{Ph(m)}: 128.26 d (J = 8.20); C^{Ph(p)}: 129.36 s; C¹: 61.96 s; C²: 44.11 s; C³: 57.67 s; C⁴: not observed; C⁵: 40.80 s; dmpC^{2,9}: 158.43 s; dmpC^{3,8}: 125.13 s; dmpC^{4,7}: 137.20 s; dmpC^{5,6}: 125.61 s; dmpC^{11,12}: 142.04 s; dmpC^{13,14}: 126.84 s; dmpC^{15,16}: 26.32 s.

2.4. DFT calculation

DFT calculations were performed using the Gaussian 09 (Rev.E.01) package [45]. We employed the M06-2X - Minnesota standalone functional with 54% HF exchange [46]. The basis sets employed were 6-311 + G(d,p) both for geometry optimization and single-point calculations, (except iodine atom, for which 6-311G(d,p) basis set [47] was used). The structures were optimized in DMSO using the Polarizable Continuum Model (PCM). Minima of energy were characterized as such by computation of the harmonic vibrational frequencies.

2.5. Cell cultures

MCF7 cell line (human breast adenocarcinoma, morphology: epithelial-like, ATCC: HTB-22), A549 cell line (human lung adenocarcinoma, morphology: epithelial, ATCC: CCL-185), and CT26 (mouse colon carcinoma, morphology: fibroblast, ATCC: CRL-2638) were cultured in Dulbecco's Modified Eagle's Medium (DMEM, Corning) with phenol red, supplemented with 10% fetal bovine serum (FBS) and with 1% streptomycin/penicillin. MCR-5 cell line (primary line of human pulmonary fibroblasts, ATCC: CCL-171) was cultured in minimum essential medium (MEM, Corning) with only 10% fetal bovine serum (FBS). Cultures were incubated at 37 °C under a humidified atmosphere containing 5% CO₂. Cells were passaged using a solution containing 0.05% trypsin and 0.5 mM EDTA. All media and other ingredients were purchased from ALAB, Poland.

2.6. Cytotoxic activity

Cytotoxicity was assessed by MTT assay performed according the protocols described elsewhere [48]. In brief, 1 × 10⁴ cells per well, seeded in 96-well flat bottom microtiter plate, were incubated with the tested complexes at various range of concentrations for 4 and 24 h. Afterwards, cell viability was determined using the Hill equation (Origin 9.0) with regard to the untreated cells (control), where y₀ – untreated cell control (which was set to 100% viability), y₁₀₀ – a lysis control (where the cells were treated with 0.5% triton X-100 was set to 0% viability, which was found to be sufficient to induce 100% cell death), IC₅₀ – values for the concentration [c] at which the viability of the cells reaches 50%, H – the Hill coefficient (describing cooperativity):

$$y = y_0 + \frac{(y_{100} - y_0 b)[c]^H}{(IC_{50})^H + [c]^H}$$

Each compound concentration was tested in five replicates and

repeated at least three times. Determined values of IC₅₀ are given as mean + S.D. (Standard Deviation).

2.7. Fluorescence microscopy

Viable and dead cells were detected by staining with fluorescein diacetate (FDA, 5 mg/L) and propidium iodide (PI, 5 mg/L) for 20 min and examined using fluorescence inverted microscope (Olympus IX51, Japan) with an excitation filter of 470/20 nm. Photographs of cells after treatment with the tested compounds were taken under magnification 20 ×.

2.8. Cell cycle analysis using flow cytometry

In order to distinguish cell death induced by studied compounds, Annexin V Apoptosis Detection Kit APC (Affymetrix) was used. The studied compounds **Sargly**, **PSG** and **1-PSG** (IC₅₀) were incubated for 24 h with tumor cells MCF7 (density 5 × 10⁵ cells/mL) in 12-well plates. After this time, the compound solutions were removed and the cells washed with PBS (phosphate-buffered saline, pH = 7,4) buffer and Binding Buffer. Trypsin was added to the cells and then they were left for 10 min at 37 °C in a humidified atmosphere containing 5% CO₂. The cells were collected, centrifuged and separated from the supernatant, then washed in 0.5 ml PBS buffer (buffer phosphate saline NaCl, KCl, Na₂HPO₄, KH₂PO₄) and again centrifuged and separated from the supernatant. Finally, Annexin V Apoptosis Detection Kit APC (Affymetrix) was applied according to manufacturer's instructions. The experiment was repeated at least 3 times. The dot-plots of the percentage distribution of individual cell populations were obtained.

2.9. Copper uptake

Cells (MRC5 or MCF7) at density of 2 × 10⁶ cells/2 mL were seeded on 6-well plates and incubated with complex **1-PSG** (c = 1 μM for 4 or 24 h) at standard conditions (37 °C, 5% CO₂). Solution of the studied compound was removed; the cells were washed twice with PBS buffer and trypsinized. Cells, for ICP-MS analysis, were mineralized in 1 mL of 65% HNO₃. Measurement of the concentration of copper ions was determined by a mass spectrometer (ELAN 6100 Perkin Elmer) with an inductively coupled plasma (ICP-MS). Protein content was assessed with Bradford Protein Assay (Thermo Scientific™) [49]. The copper content under each condition is expressed as ng Cu/mg protein. The experiment was repeated at least 3 times and results are presented as mean value + S.D.

2.10. Detection of mitochondrial membrane potential (Δψ)

Mitochondrial membrane potential (MMP) depletion was determined by JC-10 Assay (Life Technologies, USA). MCF7 cells were seeded on 96-well plates at 1 × 10⁴ cells/0.2 mL. After 24 h medium was replaced with solutions of **1-PSG** at IC₅₀ concentration as well as gentamicin (0.5 mg/mL) and ciprofloxacin (10 μg/mL) as positive and negative control, respectively. After that, cells were incubated for 24 h at standard condition (37 °C, 5% CO₂). Then, they were washed twice with PBS buffer and incubated with JC-10 for 1 h. Afterwards, emission was measured at two different excitation wavelengths (λ_{exc} = 540 nm, λ_{em} = 570 nm) and (λ_{exc} = 485 nm, λ_{em} = 530 nm). Results are presented as the intensity ratio of red to green emission (mean + S.D.).

2.11. Caspase activity assays

Colorimetric Protease Caspase-3/ CPP32 and Caspase-9/Mch6/Apaf-3 Colorimetric Protease kits (Life Technologies, USA) were used for detection of activated caspases 3 and 9, respectively. The effect of compounds on the activation of caspase 3 and 9 in MCF7 cells was monitored spectrophotometrically using the substrates DEVD-pNA and

LEHD-pNA, respectively, according to the supplier's instructions. In brief, cells at 5×10^5 cells/2 mL were seeded on 6-well plates and incubated for 24 h. Then, after medium aspiration cells were treated at IC_{50} concentration for 24 h with copper(I) complex (**1-PSG**) and etoposide (positive control, $1 \mu\text{g/mL}$) at standard condition (37°C , 5% CO_2). Afterwards, cells were trypsinized, centrifuged, and suspended in $50 \mu\text{L}$ of the cooled cell lysis buffer (Cell Lysis Buffer) for 10 min. The cell degradation products were centrifuged (1 min, $10,000 \times g$) and the supernatant was transferred to fresh Eppendorf tubes and left on ice. Concentration of isolated proteins was determined in all lysates using Bradford Protein Assay (Thermo Scientific™) [50]. $50 \mu\text{L}$ of 10 mM dithiothreitol (**DTT**) solution in reaction buffer and $5 \mu\text{L}$ of 4 mM DEVD-pNA (in the case of caspase 3) or LEHD-pNA (in the case of caspase 9) were added to 1 mg/mL of collected proteins and incubated for 2 h in the dark at 37°C . Absorbance in 96-well plates at 400 nm was measured using plate reader (200 M PRO NanoQuant; Tecan, Switzerland) (free pNA). Samples were analyzed in triplicate, and standard deviations were calculated.

2.12. DNA strand break analysis

The ability of **SarGly**, **PSG** and **1-PSG** to induce single- or double-strand breaks in plasmid DNA was tested with the pBR322 plasmid ($C = 0.5 \text{ mg/mL}$). All compounds were dissolved in **DMF** with/without: H_2O_2 ($c = 50 \mu\text{M}$), **DMSO** (10% V:V) which concentration was kept constant in the final solution. After 1 h incubation at 37°C , reaction mixtures ($20 \mu\text{L}$) were mixed with $3 \mu\text{L}$ of loading buffer (bromophenol blue in 30% glycerol) and loaded on 1% agarose gels, containing **EB**, in TBE buffer (90 mM Tris–borate, 20 mM EDTA, $\text{pH} = 8.0$). Gel electrophoresis was performed at a constant voltage of 100 V ($4 \text{ V}\cdot\text{cm}^{-1}$) for 60 min. The gel was photographed and processed with a Digital Imaging System (Syngene Biotech). For the densitometric analysis the UltraQuant 6.0 program was used.

2.13. Reactive oxygen species (ROS) production

Production of Reactive Oxygen Species (ROS) by **SarGly**, **PSG** and **1-PSG** was determined by photometric tests using: 5-(and-6)-chloromethyl-20,70-dichlorodihydrofluorescein, diacetate acetyl ester

($\text{H}_2\text{DCF-DA}$) and a Cyto-ID® Hypoxia/Oxidative Stress Detection Kit. The assay was performed in 96-well plates, where cells were seeded at a density of 1×10^4 cells/0.2 mL of medium. Acetyl ester ($\text{H}_2\text{DCF-DA}$) was prepared by dissolving it in sterile **DMSO** in anaerobic conditions. Next, the dye solution was diluted in medium with 2% serum. Medium from the cells was removed, and they were also washed using **PBS Buffer**. Dye solution at a final concentration of $1 \mu\text{M}$ was added. Cells with dye were incubated for 30 min in darkness (37°C in a humidified atmosphere containing 5% CO_2). After this time the dye solution was removed and the cells washed twice with **PBS buffer**. Solutions of studied complexes in IC_{50} and a solution of H_2O_2 (final concentration $\sim 100 \mu\text{M}$) as a positive control were added to the cells. The cells with investigated substances were incubated for 30 min, 4 and 12 h at 42°C in a humidified atmosphere containing 5% CO_2 . The emission of solution was measured at 495 nm using an Infinite 200 M PRO NanoQuant plate reader (Tecan, Switzerland). Results obtained using acetyl ester ($\text{H}_2\text{DCF-DA}$) were confirmed by results obtained using a second dye Cyto-ID® Hypoxia/Oxidative Stress Detection Kit. In this case, the cells were incubated with tested compounds for 30 min, 4 and 24 h at 37°C in a humidified atmosphere containing 5% CO_2 . After 3.5 h of incubation, ROS-inducing reagent as a positive control was added to the untreated cells. After 4 h all supernatants were removed, the cells were washed twice with **PBS buffer** and detector reagent (Oxidative Stress Detection Kit) was added. Cells with dye were incubated in standard conditions for 1 h. After this time emission spectra with excitation wavelength at 505 nm was measured. The experiment was repeated at least 3 times. The results were presented as a graph of emission intensity, which is proportional to ROS concentration at an appropriate point in time.

3. Results and discussion

3.1. Synthesis

Synthetic routes of described here compounds are presented in **Fig. 1**. Firstly, starting salt $\text{PPh}_2(\text{CH}_2\text{OH})_2\text{Cl}$, according to a literature procedure [44], and starting phosphine ligand $\text{PPh}_2\text{CH}_2\text{OH}$ (**POH**) were synthesized. **POH** and its copper(I) complexes were described in our previous papers in details [15,16]. Subsequently, we obtained a new

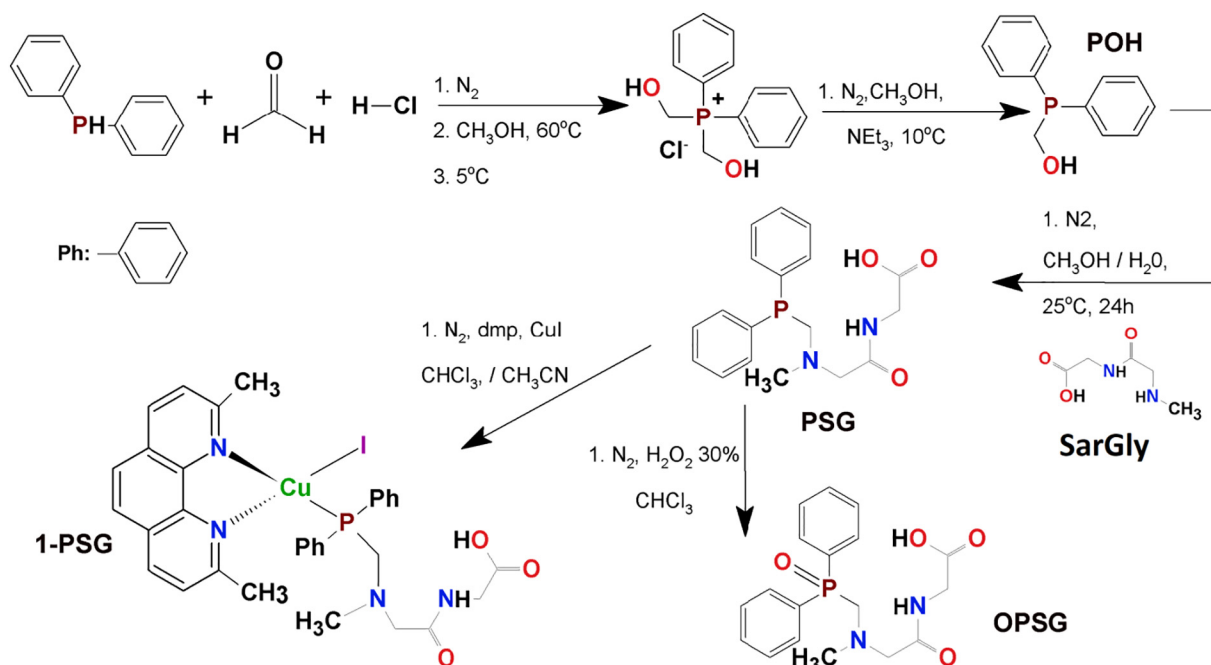


Fig. 1. Schematic view of the compounds and synthetic routes.

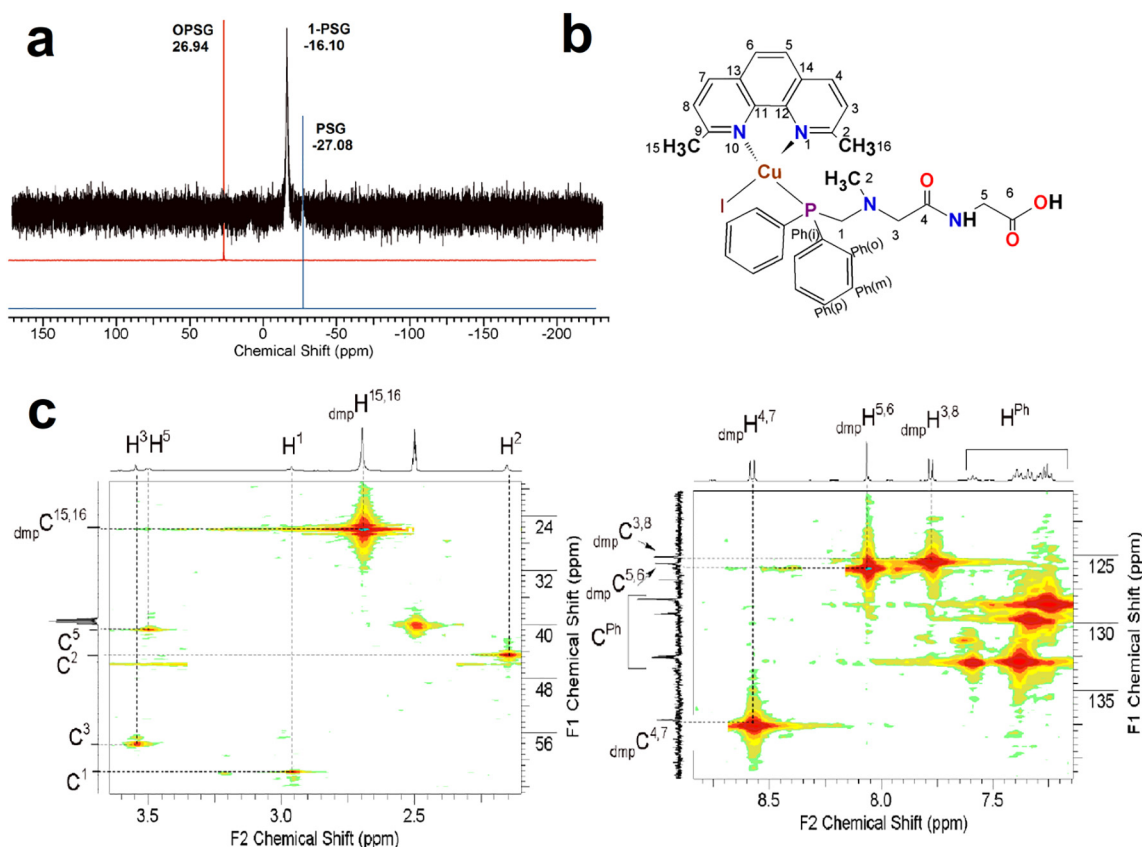


Fig. 2. (a) $^{31}\text{P}\{^1\text{H}\}$ NMR spectra (298 K, DMSO) of **PSG**, **OPSG** and **1-PSG**; (b) Scheme of **1-PSG** structures with atomic enumeration; (c) HMBC NMR spectra (298 K, DMSO) of **1-PSG**.

phosphine-peptide conjugate ($\text{PPh}_2\text{-CH}_2\text{-Sar-Gly-OH}$; **PSG**) by attachment of the peptide motif sarcosine-glycine (**SarGly**) to **POH**. In the next step, phosphine oxide ($\text{O}=\text{PPh}_2\text{-CH}_2\text{-Sar-Gly-OH}$; **OPSG**) and a new copper(I) complex [$\text{Cu}(2,9\text{-dimethyl-1,10-phenanthroline})\text{PSG}$] (**1-PSG**) was synthesized (Fig. 1).

Since phosphine oxidation is a common process during complex formation, we synthesized phosphine oxides for comparative purposes. The syntheses were carried under nitrogen, using Schlenk techniques.

3.2. Spectroscopic properties

The synthesized compounds were thoroughly characterized by NMR (1D and 2D) and UV–Vis spectroscopy. These two techniques allowed determining the structures of organic and inorganic compounds as well as stability of the **1-PSG** complex in solution. Due to the low solubility of the complex in water, their NMR spectra were recorded in DMSO ($^{13}\text{C}\{^1\text{H}\}$ NMR = 40 ppm; ^1H NMR = 2.50 ppm). All spectra and spectral data are presented in Fig. 2 and Supporting Information Figs. S1–S8 and Table S1.

Formation of phosphine ligands, their oxides and copper(I) complexes leads to significant changes in the chemical shifts and coupling constants on the NMR spectra. We have observed that phenomenon in the case of the previously obtained compounds [15,16,50,51]. In the $^{31}\text{P}\{^1\text{H}\}$ spectra, the value of the chemical shift for **POH** (the starting ligand) was equal to -9.33 ppm. After formation of **PSG** and **OPSG**, the signal moved to -27.08 and 26.94 ppm, respectively (Fig. 2A). Formation of the Cu(I) complex resulted in significant broadening and a low-field shift of the phosphine signal observed in $^{31}\text{P}\{^1\text{H}\}$ NMR spectra. The value of the chemical shift changed from -27.08 ppm for **PSG** – free phosphine to -16.10 ppm for **1-PSG** – complex (Fig. 2).

Synthesis of **PSG** and **OPSG** significantly affected the chemical shifts of dipeptide (**SarGly**) signals on the ^1H and $^{13}\text{C}\{^1\text{H}\}$ NMR spectra. After

PPh_2CH_2 -motif connection to peptide **SarGly**, strong shift of all signals on ^1H NMR spectrum towards higher fields was observed proving phosphine ligand formation (Supporting information Figs. S1–S8, Table S1). However, the strongest chemical shift for H^1 atom, after reaction of peptide with $\text{PPh}_2\text{-CH}_2\text{-OH}$ (**POH**), moved from 4.42 ppm for starting phosphine **POH** to 3.07 ppm for $\text{PPh}_2\text{-CH}_2\text{-Sar-Gly-OH}$. This phenomenon, that we expected to observe, can be explained by increasing the electron density around H^1 atom after peptide connection to starting phosphine.

As expected, the formation of the **1-PSG** affected the chemical shifts of the signals originating from the both ligands (diimine and phosphine) on the ^1H and $^{13}\text{C}\{^1\text{H}\}$ NMR spectra. The largest alterations of diimine chemical shifts were observed for the atoms neighboring the nitrogens, but number of the signals did not increase. This is a direct proof that these atoms (NN) coordinate to Cu(I) ions in a symmetrical, chelating mode. Signals $\text{dmpH}^{3,8}$, $\text{dmpH}^{4,7}$, $\text{dmpC}^{3,8}$ and $\text{dmpC}^{11,12}$ in neocuproine molecule were the most affected among all signals. In the case of **PSG**, the largest changes were observed for H^1 , H^2 , C^1 and C^{I} atoms (Supporting information Figs. S1–S8 and Table S1). What is more, signals $\text{dmpC}^{11,12}$, $\text{dmpC}^{2,9}$, PSGC^{I} , PSGC^{O} , PSGC^{m} , PSGH^1 , PSGH^2 were strongly shifted towards higher fields after coordination. This might be connected with an increase of the shielding effect resulting from the formation of coordination compound. Noteworthy, the data described here are fully compatible with the results presented in our previous papers for complexes with the phosphines derived from amines and fluoroquinolone antibiotics [15,16,24,50,51–53].

Summing, the detailed analysis of the $^{31}\text{P}\{^1\text{H}\}$, ^1H and $^{13}\text{C}\{^1\text{H}\}$, HMBC, HMQC and COSY NMR spectra showed that in the complexes, the central Cu(I) ion is tetrahedrally coordinated by two nitrogen atoms of neocuproine and the phosphorus atom of the phosphine ligand. This is a typical coordination mode for the copper(I) complexes with diimines and/or phosphines [15,16,24,50–53].

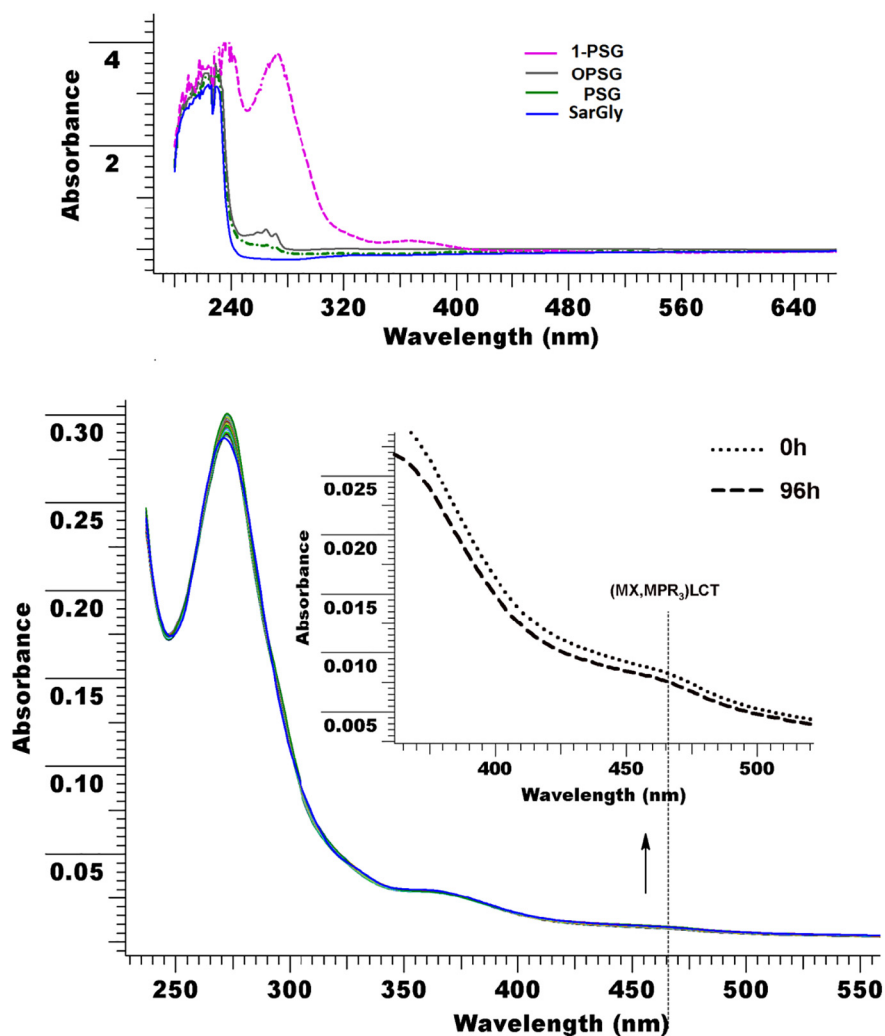


Fig. 3. Absorbance spectra in DMEM with 2% DMSO, in aerobic atmosphere (37 °C) of upper panel: SarGly, PSG, OPSG and 1-PSG; lower panel: 1-PSG after 96 h.

Electronic spectra of all compounds are presented in Fig. 3A. In case of 1-PSG characteristic absorption band ((MX,MP)₃LCT) [52,53] at 465 nm appeared. UV-Vis spectroscopy was also used to determine the stability of the 1-PSG complex (Fig. 3B). UV-Vis spectra were recorded in the presence of DMEM culture medium with 2% DMSO under aerobic conditions. During 96 h of the experiments we observed no significant reduction in the intensity of the absorption band ((MX,MP)₃LCT) [52,53]. This was clear evidence of the absence of Cu(I) to Cu(II) oxidation processes under aerobic conditions in the presence of water and confirmed the validity of the choice of the diimine ligands.

3.3. DFT calculation

Simplicity of the sarcosine-glycine (SarGly) allowed determining the most stable conformer. We analyzed 4 different conformers of anionic and zwitterionic forms and the most stable one was zwitterion stabilized by two independent hydrogen bonds. The first one was N–H...O between protonated S amine group and amide oxygen and the second one - N–H...O between amide NH group and one of the G oxygens from deprotonated carboxylate group. Other conformers had energy higher by 2.3, 5.7 and 8.7 kcal/mol.

We also determined the most stable conformer of anionic form of *N*-methylated anionic MeSarGly fragment, which is a close molecule to the –CH₂SarGly fragment in the phosphine ligand. The most stable conformer was the one with amide –NH proton in a close proximity to the sarcosine amine N atom and glycine G carboxylate O atom (Fig. 4).

To determine the most stable conformer of PSG we used the two lowest energy conformers of *N*-methylated SarGly in two positions relative to the position of the phosphorus atom. The most stable one is shown on Fig. 4 DFT geometries of two of the lowest energy conformers are described in Table 1. They are characterized by similar P–C bond lengths and bond angles around phosphorus atom expressed as S4 parameter (see explanation under the Table 1.) and the same conformations of the –SG moiety.

The main difference between them is the orientation of the –SarGly moiety. For the lowest energy conformer (a) the N–C₂H₃ bond is “antiparallel” to the artificial P–LP bond with $\alpha(X-P\cdots N1-C2) = 174.79^\circ$ (Table 1) while for the (b) conformer this angle equals to 19.55°. Analogously, we determined the most stable conformer of the phosphine oxide OPSG. Interestingly, for the OPSG (b) conformer is the lowest energy one, but the energy difference is only 0.8 kcal/mol. For both lowest energy conformers, P–C bonds are significantly shortened and S4 values are much smaller, indicating large changes in the geometries caused by the presence of the electron-withdrawing oxygen atom strongly bound to P atom, what follows the trend observed for the trisaminomethylphosphines [54] and diphenylaminomethylphosphines derived from sparfloxacin and ciprofloxacin [17].

Determining of the structure of the 1-PSG complex was more complex and involved analysis of three parts of the molecule: orientation of the –Ph rings relative to the dmp ring, conformation and position of the –CH₂SarGly fragment. Geometries of the 3 lowest energy isomers is listed in Table 1 and the views of their molecules are shown in Fig. 5.

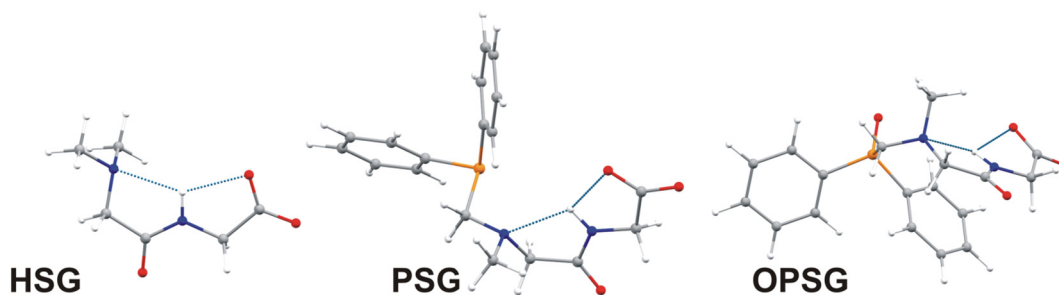


Fig. 4. The most stable conformers of *N*-methylated HSG anion, phosphine PSG and its oxide OPSG.

As expected, all calculated isomers of **1-PSG** show a distorted tetrahedral geometry around copper(I) central ion. Although the value of α (the angle between the plane of the dmp ligand and the plane formed by Cu, I and P) in most cases is close to 90° , the angles between dmp plane and Cu–P and Cu–I bonds differ significantly. Like for the analogous CuI complex with dmp and with diphenylphosphinomethyl derivative of sparfloxacin [16], for the **1-PSG** complex the most stable isomers are those with one of the phosphine –Ph rings overlapping the dmp ligand. It should be noted however, that apart from the high energy isomers with fragment $-\text{CH}_2\text{SarGly}$ overlying dmp ligand, the relative energies of other isomers did not exceed $+5.2$ kcal/mol. For **1-PSG-a** – the lowest energy isomer the angle between the –Ph and dmp planes is only 7.53° and the distance between the –Ph centroid to the dmp plane is 3.277 \AA . For the phosphine ligand, impact of the coordination to Cu(I) ion on the geometry around phosphorus atom is pronounced mainly by the diminution of the $S4$ value by 10–12, but the P–C bonds are not shortened, probably due to steric hindrances caused by the –Me groups from the dmp ligand. The three isomers presented here differ strongly by orientation of the $-\text{CH}_2\text{SG}$ fragment, but in each of three lowest energy isomers conformation of the –SG moiety is close to its conformations in organic molecules. The largest discrepancy is observed for isomer (a), where one of oxygen atoms from the carboxylate groups is placed in a short contact not only with the amide proton but also a proton from the $-\text{CH}_2-$ group and proton from the –Ph ring (Fig. 5).

3.4. Cytotoxicity

Cytotoxicity of the synthesized complex (**1-PSG**), peptide (**SarGly**), peptide-phosphine conjugate (**PSG**) and its oxide (**OPSG**), starting compounds (dmp and CuI) and cisplatin was tested *in vitro* against three cancer cell lines: mouse colon carcinoma (CT26), human lung adenocarcinoma (A549) and human breast adenocarcinoma (MCF7) as well as one primary line of human pulmonary fibroblasts (MRC-5). We

decided to choose the murine cancer cell line because of its biological and pharmacological properties, which are representative of the properties of human colon carcinoma [55]. We have chosen these types of the cells to our investigation because recently published statistics has shown that for the past two decades lung cancer has ranked the first, colon cancer – the second and breast cancer – the third place in terms of morbidity [55].

Most of the studied here compounds are insoluble in aqueous media. Therefore, all of them were predissolved in DMSO (maximum final concentration 0.2% V:V [56]) for the biological tests. The final compounds concentration ranged from 0.1 to 0.001 mM. Cytotoxic activity was assessed on the basis of IC_{50} values (concentration of a drug required to inhibit the growth of 50% of the cells [57]). IC_{50} values were determined from the plots of cell viability in the presence of each compound; matching dose–response curves calculated using the Hill equation (Origin 9.0) [48]. The values of IC_{50} were confirmed by an analysis of images of the stained tumor cells treated with the compounds at the corresponding concentrations (Table 2 Fig. 6). The cell viability was examined by counting the green cells (fluorescein diacetate – FDA stain) with normal nuclei, which were considered to be the surviving cells, and the red ones (propidium iodide – PI stain) considered to be dead.

For the comparison purposes we showed also results previously obtained by our group (published experiments for those compounds were performed in the same conditions as presented here data in our laboratories) for **POH** ($\text{PPh}_2\text{CH}_2\text{OH}$), **OPOH** ($\text{OPPh}_2\text{CH}_2\text{OH}$), **1-POH** ($\text{Cu}(\text{dmp})\text{PPh}_2\text{CH}_2\text{OH}$), sparfloxacin (**HSf**, a 3rd generation quinolone), **PSf** ($\text{PPh}_2\text{CH}_2\text{Sf}$), **OPSF** ($\text{OPPh}_2\text{CH}_2\text{Sf}$) and **1-PSf** ($\text{Cu}(\text{dmp})\text{PPh}_2\text{CH}_2\text{Sf}$) (Table 2) [15,16].

Peptide (**SarGly**), phosphine ligand (**PSG**) and its oxide (**OPSG**) did not show any activity towards investigated cancer cell lines even after incubation time prolongation (4 h \rightarrow 24 h) (Table 2) in order to **1-PSG** complex which exhibited the highest cytotoxic activity among all studied compounds (Supporting Information Table S2). Activity of this

Table 1

DFT (M06-2X/6–311 + G(d,p)) relative energies and geometries for the lowest energy conformers of PSG, OPSG and 1-PSG.

	PSG-a	PSG-b	OPSG-a	OPSG-b	1-PSG-a	1-PSG-b	1-PSG-c
E(rel) [kcal/mol]	0	1.28	0.81	0	0	1.18	1.14
$\alpha(\text{P-C1-N1-C2})$	161.75	79.30	156.65	102.28	–75.04	73.89	–57.77
$\alpha(\text{X-P...N1-C2})^a$	–174.79	19.55	–169.94	23.72	–120.85	8.37	–75.66
av.(P-C)	1.8530	1.8547	1.8220	1.8232	1.8521	1.8434	1.8553
$S4^b$	53.34	52.41	24.43	21.68	42.95	38.37	40.25
P–O			1.5064	1.5064			
P–Cu					2.4584	2.4543	2.4854
Cu–I					2.6778	2.6754	2.6802
P–Cu–I					124.16	124.68	121.33
α^c					86.78	87.48	80.31

^a Torsion angle between N–CH₃ bond and P–O, P–Cu bonds or LP–P – an artificial vector in the direction of the lone electron pair on P atom, generated to obey condition: $\alpha(\text{X-P-C}^1) = \alpha(\text{X-P-C}^{\text{Ph-i}}) = \alpha(\text{X-P-C}^{\text{Ph-i}})$.

^b Symmetric deformation coordinate – the difference between the sum of the angles between the substituents and the X and the angles between substituents ($S4 = \text{XPC}^{\text{Ph-i}} + \text{XPC}^{\text{Ph-i}} + \text{XPC}^1 - \text{C}^1\text{PC}^{\text{Ph-i}} - \text{C}^1\text{PC}^{\text{Ph-i}} - \text{C}^{\text{Ph-i}}\text{PC}^{\text{Ph-i}}$) – see [24, 54] for full details.

^c α – the angle between the plane of the dmp ligand and the plane formed by Cu, I and P atoms [24].

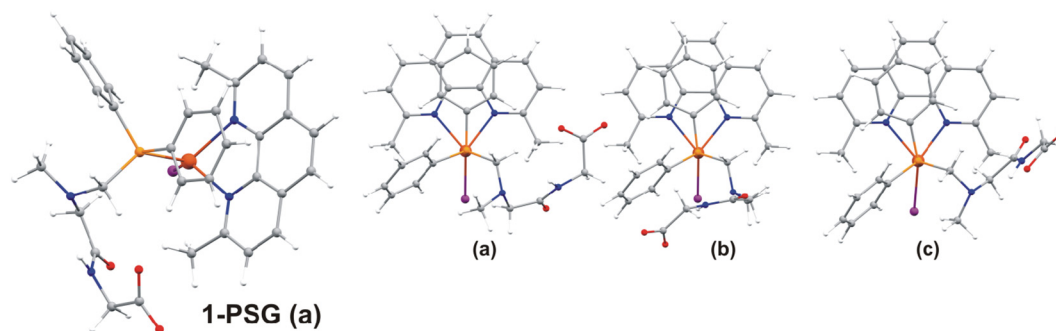


Fig. 5. UP: The structure of the lowest energy isomer of **1-PSG** complex determined using DFT methods. DOWN: the structures of $-a$, $-b$, and $-c$ isomer – view along P–Cu bond.

complex was slightly higher after 24 h of incubation comparing to 4 h regarding to all studied lines. The significant increase of **1-PSG** activity after the time prolongation (4 h \rightarrow 24 h) was observed for MCF7 cancer line (six times). What is more, **1-PSG**, comparing to literature complexes with metal ions such as: Pt, Ru, Cu, Ir, Zn, Pd, seems to show the best cytotoxic activity towards A549, CT26 and MCF7 with small exceptions (Supporting Information Table S2 with the literature references). For instance, copper(I) complex $\text{Cu}(\text{dppe})(2,2'\text{-bipy})[\text{BF}_4]$ exhibited activity twice higher against MCF7 [59] comparing to described here complex, but there is no any information about its toxicity towards normal cell lines. What is more, exchanging of fluoroquinolone molecule in **1-PSf** complex (Table 2) to simple dipeptide motif (**SarGly**) resulted in increase of the copper(I) complex cytotoxicity.

Tests employing normal line (MRC-5) showed that **SarGly**, **PSG** and **OPSG** were not toxic as opposed to cisplatin and literature complexes (Table S2). Unexpectedly, toxicity of **1-PSG** was significantly lower (more than two times) than cisplatin and literature complexes with copper(I) ions (**1-POH**, **1-PSf** Table 2). Calculated values of therapeutic index (TI) for **1-PSG**, **1-POH** and **1-PSf** (Table 2) clearly indicated that **1-PSG** could be a perfect candidate as anticancer drug, since it exhibited high cytotoxicity against studied cancer cells and low toxicity towards healthy line. Value of TI obtained for **1-PSG** was the highest for MCF7 line. What is worth emphasizing that exchanging of

fluoroquinolone molecule from copper(I) complex (**1-PSf**, Table 2) to simple dipeptide motif (**SarGly**) resulted in significant decrease of the copper(I) complex toxicity towards normal cells MRC5.

We decided to perform detailed study to understating action mode of **1-PSG** complex. It was clearly seen that **1-PSG** is the most active against MCF7 cancer cell line. Due to, human breast adenocarcinoma was selected to our further investigation (Table 2).

3.5. Cellular uptake

In an attempt to correlate cytotoxicity with the cellular uptake of the tested complex, the copper content was evaluated for MCF7 and MRC5 cells treated for 4 and 24 h with **1-PSG** in the same concentration ($C = 1 \mu\text{M}$). Only one concentration ($1 \mu\text{M}$) has been selected in our research to see differences in delivery of **1-PSG** to cancer and normal cells. As we have postulated that short peptides (*i.e.* **SarGly**) can be used as selective carriers of copper(I) complexes into the cancer cells, performing copper uptake experiments in the same concentration of compound, for healthy and cancer cells, was crucial. The intracellular copper amount was quantified by ICP-MS analysis and is expressed as ng Cu per mg of cellular protein (Fig. 7). The experiment was repeated at least 3 times and values Cu concentrations are presented as mean value + S.D. (standard division) in Table S3 Supplementary materials.

Table 2

IC_{50} [μM] (concentration of a drug required to inhibit the growth of 50% of the cells) values for CT26, A549, MCF7, MRC-5 cell lines after 4 and 24 h treatment with the **SarGly**, **PSGO**, **1-PSGO**, **dmp**, **CuI**, cisplatin and literature data obtained for complexes with different metal ions and ligands. Selected TI (therapeutic index) values for **1-PSG** and literature complexes **1-POH**, **1-PSf**.

	IC_{50} [μM] \pm SD			IC_{50} [μM] \pm SD			
	4 h			24 h			
	CT26	A549	MCF7	CT26	A549	MCF7	MRC5
POH	74.47 ± 1.1^a	73.98 ± 1.3^a	> 100	70.70 ± 5.5^a	74.36 ± 1.3^a	> 100	> 100
OPOH	67.54 ± 1.3^a	61.34 ± 1.1^a	> 100	59.12 ± 2.6^a	61.80 ± 1.2^a	> 100	> 100
1-POH	30.76 ± 1.1^a	31.15 ± 6.4^a	76.89 ± 5.2	46.86 ± 4.2^a	26.15 ± 6.3^a	56.32 ± 2.1	30.21 ± 0.12
TI	–	–	–	0.7	1.2	1.9	–
(1-POH)							
PSf	238.97 ± 16.8^a	163.23 ± 5.1^a	> 100	264.28 ± 12.1^a	104.08 ± 3.3^a	338.00 ± 20.7^b	> 100^b
OPSF	51.03 ± 1.2^a	74.90 ± 1.4^a	64.22 ± 2.3	109.23 ± 8.8^a	52.72 ± 9.2^a	55.02 ± 0.5^b	46.97 ± 2.8^b
1-PSf	7.33 ± 0.1^a	6.04 ± 0.1^a	8.23 ± 1.7	8.29 ± 0.7^a	7.84 ± 0.2^a	6.67 ± 0.4^b	29.64 ± 2.4^b
TI	–	–	–	3.6	3.8	4.4	–
(1-PSf)							
SarGly	> 100	> 100	> 100	> 100	> 100	> 100	> 100
PSG	> 100	> 100	> 100	> 100	> 100	> 100	> 100
OPSG	> 100	> 100	> 100	> 100	> 100	> 100	> 100
1-PSG	4.24 ± 0.8	2.13 ± 0.5	6.23 ± 8.2	3.12 ± 0.1	2.01 ± 0.2	0.98 ± 0.2	78.56 ± 1.1
TI	–	–	–	25.2	39.1	80.2	–
(1-PSG)							
dmp	64.74 ± 1.3^a	61.66 ± 1.9^a	76.23 ± 1.2	55.97 ± 4.6^a	58.12 ± 3.9^a	71.23 ± 4.2	21.34 ± 3.4
CuI	64.16 ± 3.2^a	69.95 ± 3.1^a	65.34 ± 3.1	58.23 ± 4.6^a	58.72 ± 6.4^a	60.09 ± 6.1	32.12 ± 6.6
Cisplatin	> 100	> 100	35.23 ± 2.1	> 100	> 100	50.9 ± 7.6	31.48 ± 4.1

$a^{15,51}$, b^{58} TI- therapeutic index – IC_{50} (normal cell line)/ IC_{50} (cancer cell line).

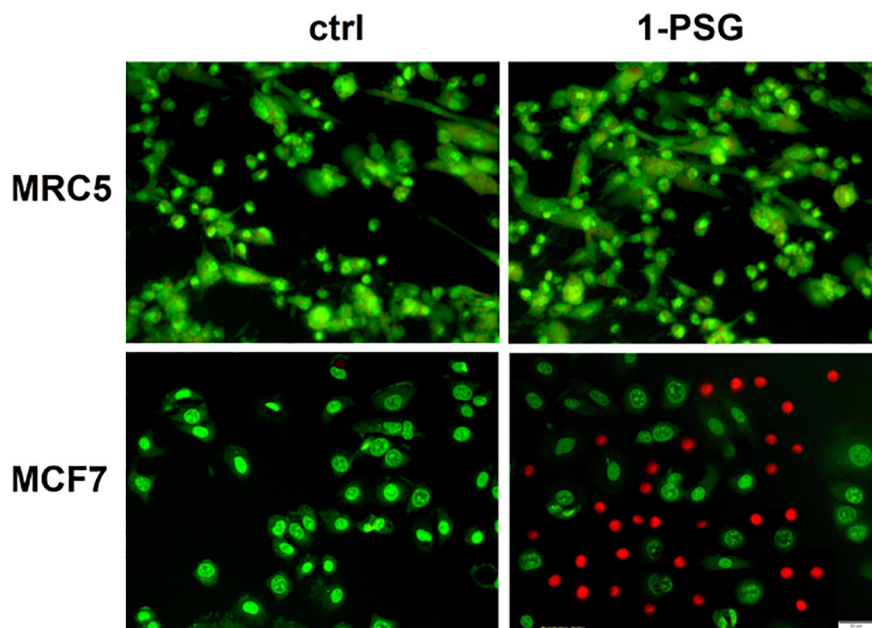


Fig. 6. The photos (magnification 20.00 ×, bar 50 μm) of MRC5 and MCF7 cell lines after 24 h incubation with and without 1-PSG in C = 1 μM. The green cells with normal morphology are viable ones (FDA), while round red cells are dead (PI).

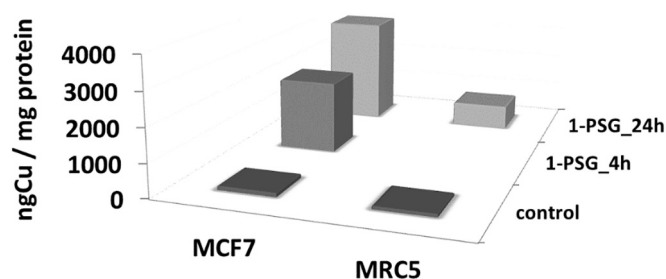


Fig. 7. Final intracellular copper concentration expressed by ng Cu/mg protein for complex 1-PSG in c = 1 μM: after 4 or/and 24 h of incubation with cancer line MCF7 or normal line MRC5.

In each studied line after incubation with 1-PSG, a significant increase of copper complex accumulation was detected over control cells (Fig. 7).

Treatment of studied cancer cells with the tested copper complex resulted in a marked time-dependent intracellular copper accumulation. After 4 h of incubation cells with 1-PSG, we noticed that 58% of starting copper concentrations penetrated into the cells. With prolongation of incubation time, copper uptake significantly increased (58% → 96%) (Fig. 7). This phenomenon can be directly connected with cytotoxicity of investigated complex (Table 2). Both: cytotoxicity and intracellular accumulation of 1-PSG, increased after prolongation of the incubation time. Also, the accumulation of copper for cancer line MCF7 and normal line MRC5 significantly differed. In the case of normal cell line MRC5 only 20% of copper accumulation was noticed (while 96% for MCF7 line was calculated; Fig. 7). Those results perfectly support the difference between cytotoxic activity of 1-PSG against MCF7 ($IC_{50} = 0.98 \pm 0.2 \mu\text{M}$) and MRC5 line ($IC_{50} = 78.56 \pm 1.1 \mu\text{M}$). What is noteworthy, cytotoxicity of this complex depends on copper intracellular accumulation. Therefore, we can postulate that high selectivity of 1-PSG can be directly connected with peptide motif (-Sar-Gly-OH). Furthermore, in literature, a motif ^{11}C -glycylsarcosine (^{11}C -Gly-Sar), was described as highly selective to the PEPTs expressed on human cancer cells [41,42]. However, this phenomenon, undoubtedly, needs further detailed investigation.

3.6. Mitochondrial membrane potential and caspases activity

Cell death has been classified into two main types: programmed cell death (PCD) and passive (necrotic) cell death. In turn, PCD can be divided into three main types: apoptosis, autophagy and non-lysosomal vacuolated degeneration – known as oncosis and paraptosis [64]. So far it was proven that copper(I) complexes mostly cause cancer cells death in two ways: apoptotic and paraptotic [15,16,49,51,58,60–62].

Paraptosis is a recently discovered type of PCD, characterized by cytoplasmic vacuolization derived from endoplasmic reticulum and/or mitochondria swelling, caspase independent, lack of apoptotic morphology, lack of DNA fragment and poly (ADP-ribose) polymerase (PARP) cleavage and ROS generation [63–66].

Apoptosis is PCD and an important self-regulatory mechanism for multicellular organisms to maintain homeostasis [64–66]. It worth mentioning, that causing apoptosis has become very important in anticancer drug research. There are two main pathways connected with apoptosis mediated by (i) cell death receptor (extrinsic pathway) and (ii) mitochondrion (intrinsic pathway). Both of them lead to activation of caspases cascade [61–66]. The second pathway is mainly associated with the delivery of cytochrome c into cytosol and activation of caspase-9. Mitochondria play a vital role in this apoptosis pathway. After that cytochrome c activates the caspase-9 initiator. In this process apoptosome is generated what, subsequently leading to activate caspase-3 (responsible for apoptotic death) [63–66].

For more precise determination of the mode of observed cell death flow cytometry with Fluorescence-Activated Cell Sorting (FACS) was applied. We performed an Annexin V/PI assay and quantitatively evaluated the apoptosis-inducing ability of the studied compounds (SarGly, PSG and 1-PSG). At the early stage of apoptosis the flipped phosphatidylserine of cytoplasmic membrane becomes available on the cell surface for binding to Annexin V. Together with propidium iodide (PI), which stains only dead cells with disintegrated membrane, Annexin V enables distinguishing cells undergoing different types of cell death [15]. The percentage of live, apoptotic as well as necrotic cells upon treatment with the compounds (IC_{50}) is presented in Fig. 8.

Data analysis proved that treatment of the MCF7 cells with SarGly, PSG and 1-PSG resulted in the vast majority of the population of apoptotic cells appearing, in opposite to necrotic ones present in

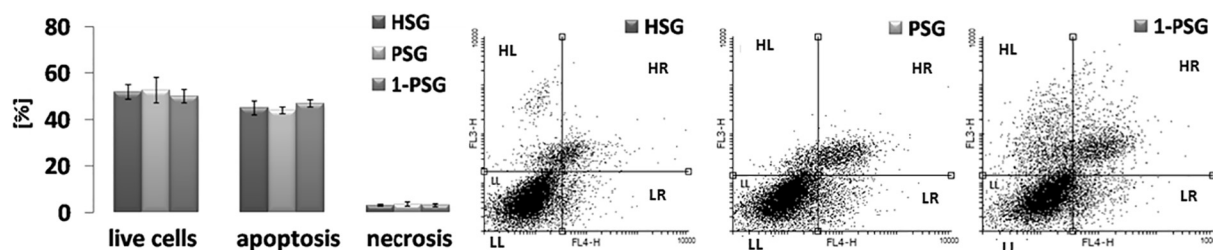


Fig. 8. On the left: percentage [%] of normal, apoptotic and necrotic cells after 24 h of incubation of MCF7 cell line with SarGly, PSG and 1-PSG in IC₅₀. on the right: scatter plots (LL – live cells, HL – early apoptotic cells, HR – late apoptotic cells, LR – necrotic cells).

minority (around 2%) (Fig. 8). We did not notice differences between organic and inorganic compounds.

As it was mentioned above, we proved that 1-PSG can be accumulated inside the cells. That is why we suspected that intrinsic pathway of apoptotic death could be the most probable in this case. For a precise determination of the MCF7 cell death type caused by 1-PSG, and better explanation of the mechanism of this process, the following experiments were carried out: (i) the measurement of the level of mitochondrial membrane potential (MMP), that decreases during apoptosis [67] and (ii) the examination of the proteolytic activity of caspases 9 and 3.

Depletion of mitochondrial potential was evaluated on MCF7 cells treated with 1-PSG by JC-10 Mitochondrial Membrane Potential Assay. JC-10 probe allows for quantitative detection of mitochondrial membrane potential (MMP) changes, considering the shift from orange to green fluorescence emission, and variation in its intensity ratio. Gentamicin, which causes an increase of MMP [68] and ciprofloxacin with its opposite effect on MMP [69] were used as a positive and a negative control, respectively.

As it is clearly seen on Fig. 9A, studied complex 1-PSG significantly decreased MMP. The level of MMP after treatment with 1-PSG is much lower than after treatment with ciprofloxacin. This means that studied complex caused increase of permeability of the mitochondrial membrane. What is interesting, in case of A549 and CT26 cells, it was noted that previously described by us complexes, mentioned above 1-PSf (Cu(dmp)PPh₂CH₂-sparfloxacin) [15], 1-PCp (Cu(dmp)PPh₂CH₂-ciprofloxacin) and 1-PNr (Cu(dmp)PPh₂CH₂-norfloxacin) [62] also caused decrease of MMP but in lower level than that was described here.

Decrease in MMP leads to the release of cytochrome c into the cytoplasm. Cytochrome c, in the presence of ATP, interacts with the Apaf-1 factor and praspaspase 9. This interaction usually triggers a cascade of executive caspases (especially caspase 3 responsible for apoptotic cell death [69,70]). Our investigation clearly shows that copper(I) complex 1-PSG activated caspase 9 (an initiator caspase) and caspase 3 (an executioner caspase) what is presented on Fig. 9B. Measured level of both caspases after treatment of MCF7 cells with 1-PSG is much higher comparing to control samples – untreated cells without compound and treated with etoposide. Concentration of caspase 3 after treatment with

1-PSG is lower than caspase 9. This allows supposing that the tested tumor cells can activate the deactivation mechanisms of this pathway of cellular death after treatment with 1-PSG [58,71].

Taking into account obtained results we can postulate, that, studied copper(I) complex 1-PSG cause controlled “cell suicide” (apoptotic death) of MCF7 cancer cells. This means that tested compound initiates cell death, which is natural and safe for the body, and above all, does not, in contrast to necrosis, cause inflammation [67]. At the current stage of the study it can be supposed that the induction of apoptosis in the examined cells probably occurs *via* caspase-dependent mitochondrial pathway.

3.7. Reactive oxygen species and DNA cleavage

Reactive oxygen species (ROS) can be produced in physiological processes occurring in the cells or generated as a result of external factors such as drugs, ultraviolet, ionizing radiation or metal ions and complexes [72,73]. Elevated levels of ROS in turn may cause cell cycle arrest or lead to the apoptosis process [74]. Furthermore, mitochondrial ROS can be produce in a very early stage before breakdown of mitochondrial membrane potential, which in turn results in releasing the pro-apoptotic factors or the activation of the other cell death mechanisms [49,61,62,74].

Cellular ROS production in MCF7 cells upon 24 h treatment with HSG, PSG and 1-PSG (IC₅₀) was monitored by H₂DCF-DA (λ_{ex} = 495 nm, λ_{em} = 530 nm) the fluorescent ROS probe. In addition, the level of oxidative stress induced by the total ROS production was also determined using a cyto-ID hypoxia/oxidative stress detection kit (λ_{ex} = 505 nm, λ_{em} = 524 nm). H₂O₂ and pyocyanin were used as positive controls in the first and second cases, respectively. The dependence of the fluorescence intensity proportional to the concentration of ROS and oxidative stress on time (three different time incubation 4, 12 and 24 h) are presented on Fig. 10.

Our studies have proved that the investigated complex 1-PSG (Fig. 10) exhibited the ability to induce ROS production inside the treated cells MCF7. Both performed tests showed that studied complex was able to induce ROS generation at a significantly higher level than

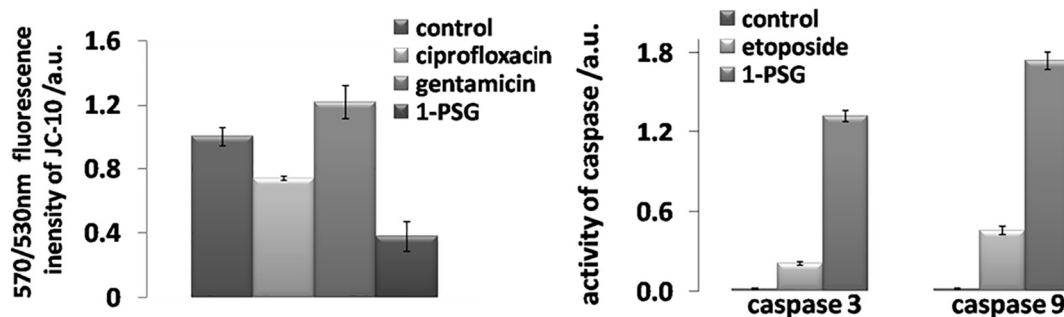


Fig. 9. Left panel: Influence of studied complex 1-PSG on intensity of JC-10 fluorescence in treated MCF7 cells. Alteration in MMP is given as an emission ratio 570 nm/530 nm. (control – untreated cells, ciprofloxacin – a negative control, gentamicin – a positive control); right panel: Influence of 1-PSG on activation of caspase 3 and caspase 9 in MCF7 cell line. As a positive control etoposide (1 μg/mL) was used.

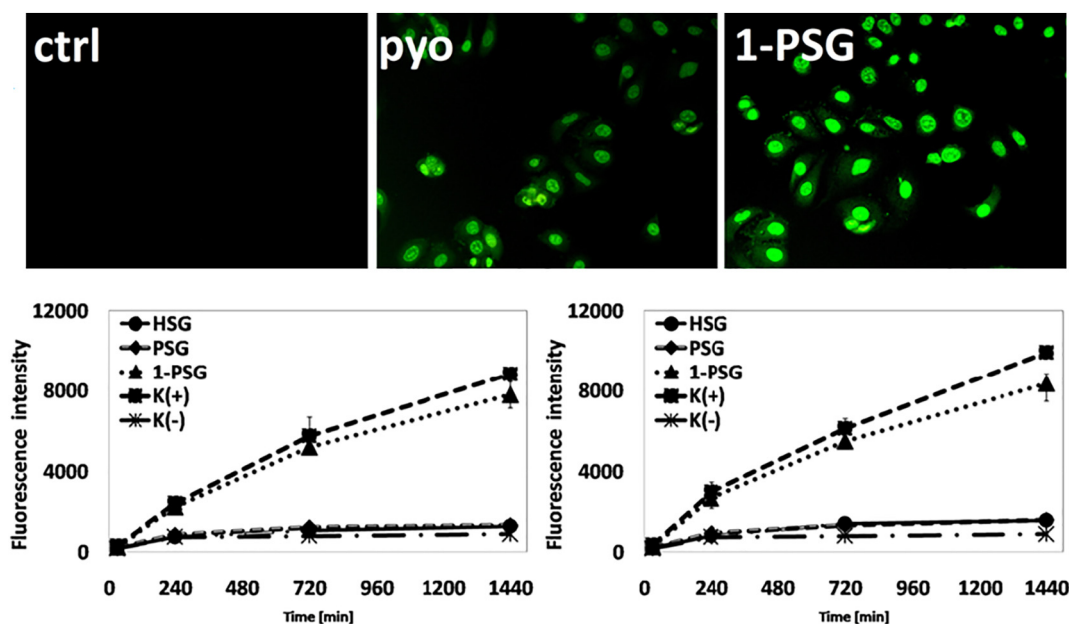


Fig. 10. Upper panel: Photos of MCF7 cells after 24 h treatment and without and with **1-PSG** or pyo (pyocyanin) for cyto-ID hypoxia/oxidative stress detection kit ($\lambda_{ex} = 505 \text{ nm}$, $\lambda_{em} = 524 \text{ nm}$); lower panel – left: The increase of ROS production in CT26 cells after 4, 12 and 24 h using $\text{H}_2\text{DCF-DA}$ for: **1-PSG**, K(+): H_2O_2 as positive control and K(-): negative control, cell without compound; lower panel – right: Oxidative stress induced by the total ROS production in CT26 cells after 4, 12 and 24 h detected by CYTO-ID Hypoxia/Oxidative Stress Test for: **1-PSG**, K(+): pyocyanin as positive control and K(-): negative control.

pyocyanin (pyocyanin toxicity results from its ability to undergo reduction by **NAD(P)H** and subsequent generation of superoxide and H_2O_2 [75]) as well as **SarGly** and **PSG**. Moreover, we observed that, **1-PSG** cytotoxicity; copper uptake and ROS level inside MCF7 cancer cells are increasing with time (*vide supra* Table 2 and Fig. 8). This phenomenon suggests that ROS are probably primarily involved in the observed cytotoxicity and the mechanism of cell death. More precise experiments will help to explain their special contribution and kind of participation in the observed cytotoxicity.

Interestingly, published previously by us **1-PSf** [15], **1-PNr** and **1-PCp** [58] generated significantly lower level of ROS in A549 and CT26 cells. Performed tests showed that **1-PSf** complex and the corresponding ligands were able to induce ROS generation at a similar level and independently of the type of cell line [15]. It means that ROS generation was not the most crucial in the observed mechanism of actions of those complexes (**1-PSf**, **1-PNr**, **1-PCp**). However, it was proven by cyclic voltammetry that **1-PSf** can act as an efficient participant in redox reactions, e.g., ROS generation that are responsible for the oxidative damage of many important cell elements and subsequent disturbances in vital processes [58]. Furthermore, copper(I) complex $\text{Cu}(\text{dppe})(2,2'\text{-bipy})[\text{BF}_4]$, mentioned above, displayed higher cytotoxicity than **1-PSG** (Supplementary materials Table S2), in the ovarian cells induced rapid production of reactive oxygen species probably through mitochondrial pathways [59].

The gel electrophoresis of pBR322 plasmid (naturally occurring as a covalently closed superhelical form (form I)) was applied to determine the ability of **SarGly**, **PSG**, **1-PSG** to induce single- and/or double-strand damage to DNA. This can lead to the formation of the relaxed/nicked (form II) and linear (form III) forms. The degree of DNA degradation was determined in a wide range of concentrations (from 0.5 to 5000 μM) (Fig. 11A). It should be emphasised that **SarGly** and **PSG** did not cause any DNA degradation (data not shown), even in concentrations exceeding the IC_{50} (5000 μM). The **1-PSG** complex, similarly to ligands, did not lead to the formation of the single- and/or double-strand DNA damage even in concentrations up to 200 μM (IC_{50} is 200 times lower). Only in concentrations over 500 μM relaxed/nicked of nucleic acid was observed. What is more, amount of form II increased along with concentration increase of **1-PSG** (Fig. 10A). In our previous paper [15] describing DNA degradation by **1-PSf**, forms I and II in concentration 10 μM were observed. Single-strand DNA damage with total decline of superhelical form was noticed at concentration equal 100 μM . This means that complex **1-PSG** is much less genotoxic than **1-PSf**.

In the presence of transition metal ions and their complexes, an endogenous oxidant H_2O_2 could be a source of hydroxyl radicals, the most powerful DNA oxidants [15,58]. As above-mentioned, **1-PSG** generated high level of ROS and therefore we decided also to check the influence of the studied complex on DNA damages. **1-PSG** presumably decomposed H_2O_2 in a free radical reaction, which can cause DNA

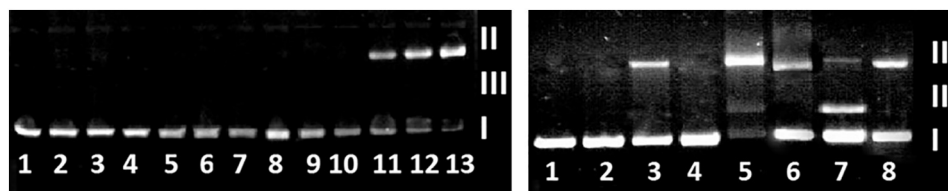


Fig. 11. Left panel: Agarose gel electrophoresis of pBR322 plasmid cleavage by **1-PSG** in a DMF (each in the 10% DMF) solution. Lanes: 1, plasmid – control; 2, plasmid + 0.5 μM **1-PSG**; 3, plasmid + 1 μM **1-PSG**; 4, plasmid + 5 μM **1-PSG**; 5, plasmid + 10 μM **1-PSG**; 6, plasmid + 20 μM **1-PSG**; 7, plasmid + 30 μM **1-PSG**; 8, plasmid + 50 μM **1-PSG**; 9, plasmid + 100 μM **1-PSG**; 10, plasmid + 200 μM **1-PSG**; 11, plasmid + 500 μM **1-PSG**; 12, plasmid + 1000 μM **1-PSG**; 13, plasmid + 5000 μM **1-PSG**; right panel: Agarose gel electrophoresis of pBR322 plasmid cleavage by **1-PSG** in a DMF (each in the 10% DMF) solution. Lanes: 1, plasmid + 10% DMSO; 2, plasmid + 1 μM **1-PSG**; 3, plasmid + 1 μM **1-PSG** + 50 μM H_2O_2 ; 4, plasmid + 1 μM **1-PSG** + 50 μM H_2O_2 + 10% DMSO; 5, plasmid + 50 μM **1-PSG** + 50 μM H_2O_2 ; 6, plasmid + 50 μM **1-PSG** + 50 μM H_2O_2 + 10% DMSO; 7, plasmid + 100 μM **1-PSG** + 50 μM H_2O_2 ; 8, plasmid + 100 μM **1-PSG** + 50 μM H_2O_2 + 10% DMSO.

damage. **1-PSG** in presence of hydrogen peroxide caused distinct changes in the plasmid structure, resulting in conversion of the supercoiled plasmid to relaxed/nicked (Fig. 10B line 3) or relaxed/nicked and linear (Fig. 10B lines 5 and 7) forms dependently on complex concentration. In higher concentrations, more serious damages of nucleic acid were observed. What was proven quantitatively, addition of DMSO (effective scavenger of the hydroxyl free radical [12]) to the reaction's mixture prevented the DNA from damage (Fig. 10B lines 4, 6 and 8). Prevention of DNA lesions by DMSO confirmed a free radical mechanism of action on the plasmid degradation processes [15]. The same results were observed in case of **1-PSf**, **1-PNr** and **1-PCp** complexes [50]. We noticed that **1-PSG** caused less DNA damages in general comparing to previously described complexes (**1-PSf**, **1-PNr** and **1-PCp**).

Cells have mechanisms that repair the damage to DNA, but if damages are too severe to be repair, the cell initiates its suicidal program and dies by apoptosis. A similar reaction is triggered by inappropriately folded proteins, which may be the result of external triggers such as free radicals [76].

4. Conclusions

In this paper we presented synthesis, physicochemical and biological characterization of the derivatives of simple dipeptide, sarcosine-glycine (**SarGly**): diphenylphosphinomethyl derivative ($P(CH_2SG)Ph_2$; **PSG**), its oxide ($OP(CH_2SG)Ph_2$; **OPSG**) and copper(I) complex (**1-PSG**) with this phosphine-peptide conjugate (**PSG**). Spectroscopic and theoretical studies revealed that **PSG** strongly binds the metal ion and forms stable (also in a presence of atmospheric oxygen) tetrahedral copper(I) complex.

The cytotoxic activity of all presented here compounds and cisplatin was tested against three cancer cell lines: mouse colon carcinoma (CT26; $^{1-PSG}IC_{50} = 3.12 \pm 0.1$), human lung adenocarcinoma (A549; $^{1-PSG}IC_{50} = 2.01 \pm 0.2$) and human breast adenocarcinoma (MCF7; $^{1-PSG}IC_{50} = 0.98 \pm 0.2$) as well as one primary line of human pulmonary fibroblasts (MRC-5; $^{1-PSG}IC_{50} = 78.56 \pm 1.1$). Peptide (**SarGly**), phosphine ligand (**PSG**) and its oxide (**OPSG**) did not show significant activity towards investigated cancer cell lines in opposite to complex **1-PSG**, which exhibited the highest cytotoxicity among all studied compounds. Values of calculated therapeutic index (TI) for **1-PSG** clearly indicated that this complex is highly selective against cancer lines, especially towards MCF7 cells line, where $^{1-PSG}TI$ equals 80, and it was two and three times higher than for CT26 and A549 cancer lines, respectively.

Precise study on elucidation of cell death mechanism showed that high accumulation of this complex inside MCF7 cancer cells influences on its cytotoxicity. Importantly, intracellular **1-PSG** accumulation was much higher for cancer cells MCF7 (96%) than for normal cells MRC5 (20%). Most likely, attachment of **SarGly** to cytotoxic copper(I) complex *via* phosphine motif improved selectivity of this complex. What is more, **1-PSG** caused apoptotic cell death with simultaneous decrease of mitochondrial membrane potential level and increase of caspase-9 and caspase-3 activity in MCF7 cells. Obtained results suggest that ROS are probably primarily involved in the observed cytotoxicity of **1-PSG** and the resulting cell death. However, this needs more precise explanation, what is our current objective.

Presented here data, proved also that exchanging fluoroquinolone molecule in copper(I) complexes (they were our previous subjects of study) to simple, lipophilic molecule of peptide, significantly decrease of copper(I) complex toxicity towards normal cells and increase its cytotoxicity against cancer cells.

This design approach of highly cytotoxic copper(I) complexes with peptides carries attached *via* phosphine linker, can be very promising in anticancer therapy. This paper is beginning of our research in this scientific field.

Abbreviations

dmp	2,9-dimethyl-1,10-phenanthroline
DFT	density functional theory
CT26	mouse colon carcinoma
A549	human lung adenocarcinoma
MCF7	human breast adenocarcinoma
MRC5	human pulmonary fibroblasts
ROS	reactive oxygen species
IC ₅₀	concentration of a drug required to inhibit the growth of 50% of the cells
RGD	peptide Arg-Gly-Asp
NGR	peptide Asn-Gly-Arg
SarGly	peptide sarcosine-glycine
PET	positron emission tomography
PEPTs	H ⁺ /peptide transporters
ICP-MS	inductively coupled plasma mass spectrometry
NMR	nuclear magnetic resonance spectroscopy
CH ₃ OH	methanol
NEt ₃	trimethylamine
CHCl ₃	chloroform
CH ₃ CN	acetonitrile
DMSO	dimethyl sulfoxide
EDTA	ethylenediaminetetraacetic acid
DMEM	Dulbecco's Modified Eagle Medium
CT	charge transfer
TI	therapeutic index
FDA	fluorescein diacetate
PI	propidium iodide
S.D.	standard division
PCD	programmed cell death
ADP ribose	adenosine diphosphate ribose
PARP	Poly (ADP-ribose) polymerase
FACS	Fluorescence-Activated Cell Sorting
LL	live cells
HL	early apoptotic cells
HR	late apoptotic cells
LR	necrotic cells
MMP	mitochondrial membrane potential
ATP	adenosine triphosphate
H ₂ DCFDA	2',7'-dichlorodihydrofluorescein diacetate
NAD(P)H	nicotinamide adenine dinucleotide phosphate-oxidase
DMF	dimethylformamide
FBS	fetal bovine serum
MEM	Minimum Essential Medium Eagle
PBS	phosphate-buffered saline
DTT	dithiothreitol

Author contributions

The manuscript was written through contributions of all authors. All authors have given approval to the final version of the manuscript.

Acknowledgment

The authors gratefully acknowledge financial support from the Polish National Science Centre (Grants 2016/23/D/ST5/00269, 2017/01/X/NZ7/01148) and from Ministry of Science and Higher Education (Grants 1233/M/WCH/13 and 1500/M/WCH/15). The DFT calculations have been carried out in the Wroclaw Centre for Networking and Supercomputing (<http://www.wcss.wroc.pl>), grant no. 140. The *in vitro* research was carried out with the equipment purchased thanks to the financial support of the European Regional Development Fund in the Framework of the Polish Innovation Economy Operational Program (contract no. POIG.02.01.00-12-023/08). The authors are grateful to

Bernadeta Nowak. PhD. (Jagiellonian University in Kraków) for flow cytometry measurements.

Appendix A. Supplementary data

Supplementary data to this article can be found online at <https://doi.org/10.1016/j.jinorgbio.2018.06.009>.

References

- [1] A. Jemal, R. Siegel, E. Ward, T. Murray, J. Xu, C. Smigal, M.J. Thun, Cancer statistics 2006, *CA Cancer J. Clin.* 56 (2006) 106–130 (4. Broder H., et al., *Rev Cardiovasc Med.*, 2008, 9, 75).
- [2] A. Jemal, F. Bray, M.M. Center, J. Ferlay, E. Ward, D. Forman, Global cancer statistics, *CA Cancer J. Clin.* 61 (2011) 69–90.
- [3] D. Kakde, D. Jain, V. Shrivastava, R. Kakde, A.T. Patil, Cancer therapeutics- opportunities, challenges and advances in drug delivery journal of applied pharmaceutical, *Science* 9 (2011) 1–10.
- [4] H. Broder, R.A. Gottlieb, N.E. Lopor, Chemotherapy and cardiotoxicity, *Rev. Cardiovasc. Med.* 9 (2008) 75–83.
- [5] L.G. Ferreira, R.N. Santos, G. Oliva, A.D. Andricopulo, Molecular docking and structure-based drug design strategies, *Molecules* 20 (2015) 13384–13421.
- [6] C.A. Naughtn, Drug-induced nephrotoxicity, *Am. Fam. Physician* 78 (2008) 743–750.
- [7] M.J. Newman, J.C. Rodarte, K.D. Benbatoul, S.J. Romano, C. Zhang, et al., Discovery and characterization of OC144-093, a novel inhibitor of P-glycoprotein-mediated multidrug resistance, *Cancer Res.* 36 (2000) 216–219.
- [8] D.W. Hoskin, A. Ramamoorthy, Studies on anticancer activities of antimicrobial peptides, *Biochim. Biophys. Acta* 1778 (2008) 357–375.
- [9] T.M. Allen, Ligand-targeted therapeutics in anticancer therapy, *Nat. Rev. Cancer* 2 (2002) 750–763.
- [10] Y.L. Janin, Peptides with anticancer use or potential, *Amino Acids* 25 (2003) 1–40.
- [11] R. Starosta, A. Bykowska, A. Kyzioł, M. Plotek, M. Florek, J. Król, M. Jeżowska-Bojczuk, Copper(I) (pseudo)halide complexes with neocuproine and amino-methylphosphines derived from morpholine and thiomorpholine -in vitro cytotoxic and antimicrobial activity and the interactions with DNA and serum albumins, *Chem. Biol. Drug Des.* 82 (2013) 579–586.
- [12] C. Santini, M. Pellei, V. Gandini, M. Porchia, F. Tisato, C. Marzano, Advances in copper complexes as anticancer agents, *Chem. Rev.* 114 (2014) 815–862.
- [13] R. Starosta, A. Brzuszkiewicz, A. Bykowska, U.K. Komarnicka, B. Bażanów, M. Florek, Ł. Gadzała, N. Jackulak, J. Król, K. Marycz, A novel copper(I) complex, [Cu(2,2'-biquinoline)P(CH₂N(CH₂CH₂)₂O)₃]-synthesis, characterisation and comparative studies on biological activity, *Polyhedron* 50 (2013) 481–489.
- [14] U.K. Komarnicka, R. Starosta, A. Kyzioł, M. Plotek, M. Puchalska, M. Jeżowska-Bojczuk, New copper(I) complexes bearing lomefloxacin motif: spectroscopic properties, in vitro cytotoxicity and interactions with DNA and human serum albumin, *J. Inorg. Biochem.* 165 (2016) 25–35.
- [15] U.K. Komarnicka, R. Starosta, M. Plotek, R.F.M. de Almeida, M. Jeżowska-Bojczuk, A. Kyzioł, Copper(I) complexes with phosphine derived from sparfloxacin. Part II: a first insight into the cytotoxic action mode, *Dalton Trans.* 45 (2016) 5052–5063.
- [16] U.K. Komarnicka, R. Starosta, A. Kyzioł, M. Jeżowska-Bojczuk, Copper(I) complexes with phosphine derived from sparfloxacin. Part I – structures, spectroscopic properties and cytotoxicity, *Dalton Trans.* 44 (2015) 12688–12699.
- [17] U.K. Komarnicka, R. Starosta, K. Guz-Regner, G. Bugła-Płoskońska, A. Kyzioł, M. Jeżowska-Bojczuk, Phosphine derivatives of sparfloxacin- synthesis, structures and in vitro activity, *J. Mol. Struct.* 1096 (2015) 55–63.
- [18] G. Borkow, J. Gabbay, Putting copper into action: copper-impregnated products with potent biocidal activities, *FASEB J.* 18 (2004) 1728–1730.
- [19] J.O. Noyce, H. Michels, C.W. Keevil, Inactivation of influenza A virus on copper versus stainless steel surfaces, *Microbiology* 73 (2007) 2748–2750.
- [20] F. Lebon, N. Boggetto, M. Ledecq, F. Durant, Z. Benatallah, S. Sicsic, R. Lapouyade, O. Kahn, A. Mouithys-Mickalad, G. Deby-Dupont, M. Reboud-Ravaux, Metal-organic compounds: a new approach for drug discovery. N1-(4-methyl-2-pyridyl)-2,3,6-trimethoxybenzamide copper(II) complex as an inhibitor of human immunodeficiency virus 1 protease, *Biochem. Pharmacol.* 63 (2002) 1863–1873.
- [21] B. Dudová, D. Hudcová, R. Pokorný, M. Mikulasova, M. Palicova, P. Sega, M. Melnik, Copper complexes with bioactive ligands. II. Antimicrobial activity, *Microbiology* 47 (2002) 225–229.
- [22] R. Starosta, K. Stokowa, M. Florek, J. Król, A. Chwiłkowska, J. Kulbacka, J. Sączko, J. Skala, M. Jeżowska-Bojczuk, Biological activity and structure dependent properties of cuprous iodide complexes with phenanthrolines and water soluble tris (aminomethyl) phosphanes, *J. Inorg. Biochem.* 105 (2011) 1102–1108.
- [23] R. Starosta, M. Florek, J. Król, M. Puchalska, A. Kochel, Cooper(I) iodide complexes containing new aliphatic aminophosphine ligands and diimines—luminescent properties and antibacterial activity, *New J. Chem.* 34 (2010) 1441–1449.
- [24] R. Starosta, M. Puchalska, J. Cybińska, M. Barys, A.V. Mudring, Structures, electronic properties and solid state luminescence of Cu(I) iodide complexes with 2,9-dimethyl-1,10-phenanthroline and aliphatic aminomethylphosphines or triphenylphosphine, *Dalton Trans.* 40 (2011) 2459–2468.
- [25] C. Abu-Gnim, I. Amer, Phosphine oxides as ligands in the hydroformylation reaction, *J. Organomet. Chem.* 516 (1996) 235–243.
- [26] P. Smoleński, F.P. Pruchnik, Aminoalkylphosphines, the water-soluble chiral phosphines, *Pol. J. Chem.* 81 (2007) 1771–1776.
- [27] K. Raghuraman, K.K. Katti, L.J. Barbour, N. Pillarsetty, C.L. Barnes, K.V. Katti, Characterization of supramolecular (H₂O)₁₈ water morphology and water-methanol (H₂O)₁₅(CH₂OH)₃ clusters in a novel phosphorus functionalized trimeric amino acid host, *J. Am. Chem. Soc.* 125 (2003) 6955–6961.
- [28] D.E. Berning, B.C. Noll, D.L. DuBois, Relative hydride, proton, and hydrogen atom transfer abilities of [HM(diphosphine)₂]PF₆ complexes (M=Pt, Ni), *J. Am. Chem. Soc.* 121 (1999) 11432–11447.
- [29] S. Deshayes, M.C. Morris, G. Divita, F. Heitz, Cell-penetrating peptides: tools for intracellular delivery of therapeutics, *Cell. Mol. Life Sci.* 62 (2005) 1839–1849.
- [30] M.C. Garnett, Targeted drug conjugates: principles and progress, *Adv. Drug Deliv. Rev.* 53 (2001) 171–216.
- [31] F. Tisato, C. Marzano, M. Porchia, M. Pellei, C. Santini, Copper in diseases and treatments, and copper-based anticancer strategies, *Med. Res. Rev.* 30 (2010) 708–749.
- [32] C.F. Shaw III, Gold-based therapeutic agents, *Chem. Rev.* 9 (1999) 2589–2600.
- [33] T.M. Simon, D.H. Kunishima, G.J. Vibert, A. Lorber, Inhibitory effects of a new oral gold compound on HeLa cells, *Cancer* 44 (1979) 1965–1975.
- [34] S.J. Berners-Price, P.J. Sadler, Phosphines and metal phosphine complexes: relationship of chemistry to anticancer and other biological activity bioinorganic chemistry, *Struct. Bond.* 70 (1988) 27–102.
- [35] C.D. Buckley, D. Pilling, N.V. Henriquez, G. Parsonage, K. Threlfall, D. Scheel-Toellner, D.L. Simmons, A.N. Akbar, J.M. Lord, M. Salmon, RGD peptides induce apoptosis by direct caspase-3 activation, *Nature* 6719 (1999) 34–39.
- [36] J. Zhang, Y. Liu, B. Yuan, Z. Wang, M. Schönhoff, X. Zhang, Multilayer films with nanocontainers: redox-controlled reversible encapsulation of guest molecules, *J. Control. Release* 159 (2012) 14968–14973.
- [37] M. Sioud, A. Mobergslien, Selective killing of cancer cells by peptide-targeted delivery of an anti-microbial peptide, *Biochem. Pharmacol.* 9 (2012) 1123–1132.
- [38] S. Majumdar, T. Siahaan, Peptide-mediated targeted drug delivery, *J. Med. Res. Rev.* 32 (2012) 637–658.
- [39] E.W. Rongsheng, N. Youhong, W. Haifan, N.A. Mohamad, C. Jianfeng, Development of NGR peptide-based agents for tumor imaging, *Am. J. Nucl. Med. Mol. Imaging* 1 (2011) 36–46.
- [40] C.D. Buckley, D. Pilling, N.V. Henriquez, G. Parsonage, K. Threlfall, D. Scheel-Toellner, D.L. Simmons, A.N. Akbar, J.M. Lord, M. Salmon, RGD peptides induce apoptosis by direct caspase-3 activation, *Nature* 397 (1999) 534–539.
- [41] N.B. Nabulsi, D.E. Smith, M.R. Kilbourn, [11C]Glycylsarcosine: synthesis and in vivo evaluation as a PET tracer of PepT2 transporter function in kidney of PepT2 null and wild-type mice, *Bioorg. Med. Chem.* 13 (2005) 2993–3001.
- [42] K. Mitsuoka, S. Miyoshi, Y. Kato, Y. Murakami, R. Utsumi, Y. Kubo, A. Noda, Y. Nakamura, S. Nishimura, A. Tsuji, Cancer detection using a PET tracer, 11C-Glycylsarcosine, targeted to H1/peptide transporter, *J. Nucl. Med.* 49 (2008) 615–622.
- [43] X.-X. Zhang, H.S. Eden, X. Chen, Peptides in cancer nanomedicine: drug carriers, targeting ligands and protease substrates, *J. Control. Release* 159 (2012) 2–13.
- [44] J. Fawcett, P.A.T. Hoye, R.D.W. Kemmitt, D.J. Law, D.R. Russell, Synthesis of bis (phosphinomethyl)amines viabis(hydroxymethyl)phosphonium salts. Isolation of 9,9-bis(hydroxymethyl)-9-phosphoniabicyclo[3.3.1]nonane hydrogensulfate and chloride salts, and the crystal structures of [PPh₂(CH₂OH)₂]+ Cl⁻ and [(C₆H₁₁)₂PCH₂]₂NCH₂MePh, *Dalton Trans.* (1993) 2563–2568.
- [45] Gaussian 09, Revision E.01, M.J. Frisch, G.W. Trucks, H.B. Schlegel, G.E. Scuseria, M.A. Robb, J.R. Cheeseman, G. Scalmani, V. Barone, B. Mennucci, G.A. Petersson, H. Nakatsuji, M. Caricato, X. Li, H.P. Hratchian, A.F. Izmaylov, J. Bloino, G. Zheng, J.L. Sonnenberg, M. Hada, M. Ehara, K. Toyota, R. Fukuda, J. Hasegawa, M. Ishida, T. Nakajima, Y. Honda, O. Kitao, H. Nakai, T. Vreven, J.A. Montgomery Jr., J.E. Peralta, F. Ogliaro, M. Bearpark, J.J. Heyd, E. Brothers, K.N. Kudin, V.N. Staroverov, T. Keith, R. Kobayashi, J. Normand, K. Raghavachari, A. Rendell, J.C. Burant, S.S. Iyengar, J. Tomasi, M. Cossi, N. Rega, J.M. Millam, M. Klene, J.E. Knox, J.B. Cross, V. Bakken, C. Adamo, J. Jaramillo, R. Gomperts, R.E. Stratmann, O. Yazyev, A.J. Austin, R. Cammi, C. Pomelli, J.W. Ochterski, R.L. Martin, K. Morokuma, V.G. Zakrzewski, G.A. Voth, P. Salvador, J.J. Dannenberg, S. Dapprich, A.D. Daniels, O. Farkas, J.B. Foresman, J.V. Ortiz, J. Gioslowski, D.J. Fox, Gaussian, Inc., Wallingford CT, (2013).
- [46] Y. Zhao, D.G. Truhlar, The M06 suite of density functionals for main group thermochemistry, thermochemical kinetics, noncovalent interactions, excited states, and transition elements: two new functionals and systematic testing of four M06-class functionals and 12 other functionals, *Theor. Chem. Accounts* 120 (2006) 215–241.
- [47] K.L. Schuchardt, B.T. Didier, T. Elsethagen, L. Sun, V. Gurumoorhi, J. Chase, J. Li, T.L. Windus, Basis set exchange: a community database for computational sciences, *J. Chem. Inf. Model.* 47 (2007) 1045–1052.
- [48] J. Weyermann, D. Lochmann, A. Zimmer, A practical note on the use of cytotoxicity assays, *Int. J. Pharm.* 288 (2005) 369–376.
- [49] S. Tardito, A. Barilli, I. Bassanetti, M. Tegoni, O. Bussolati, R. Franchi-Gazzola, C. Mucchino, L. Marchiò, Copper-dependent cytotoxicity of 8-hydroxyquinoline derivatives correlates with their hydrophobicity and does not require caspase activation, *J. Med. Chem.* 55 (2012) 10448–10459.
- [50] A. Bykowska, R. Starosta, J. Jeziarska, M. Jeżowska-Bojczuk, Coordination versatility of phosphine derivatives of fluoroquinolones. New CuI and CuII complexes and their interactions with DNA, *RSC Adv.* 5 (2015) 80804–80815.
- [51] U.K. Komarnicka, R. Starosta, A. Kyzioł, M. Plotek, M. Puchalska, M. Jeżowska-Bojczuk, New copper(I) complexes bearing lomefloxacin motif: spectroscopic properties, in vitro cytotoxicity and interactions with DNA and human serum albumin, *J. Inorg. Biochem.* 165 (2016) 25–35.
- [52] R. Starosta, A. Brzuszkiewicz, A. Bykowska, U.K. Komarnicka, B. Bażanów, M. Florek, Ł. Gadzała, N. Jackulak, J. Król, K. Marycz, A novel copper(I) complex,

- [53] R. Starosta, U.K. Komarnicka, M. Puchalska, M. Barys, Solid state luminescence of copper(I) (pseudo)halide complexes with neocuproine and aminomethylphosphanes derived from morpholine and thiomorpholine, *New J. Chem.* 36 (2012) 1673–1683.
- [54] R. Starosta, B. Bażanów, W. Barszczewskic, Chalcogenides of the aminomethylphosphines derived from 1-methylpiperazine, 1-ethylpiperazine and morpholine: NMR, DFT and structural studies for determination of electronic and steric properties of the phosphines, *Dalton Trans.* 39 (2010) 7547–7555.
- [55] a R.L. Siegel, K.D. Miller, A. Jemal, *Cancer statistics*, *Cancer J. Clin.* 2015 (65) (2015) 5–29;
b M.G. Brattain, J. Strobel-Stevens, D. Fine, M. Webb, A.M. Sarrif, *Cancer Res.* 40 (1980) 2142.
- [56] Z. Liu, L. Salassa, A. Habtemariam, A.M. Pizarro, G.J. Clarkson, P.J. Sadler, Contrasting reactivity and cancer cell cytotoxicity of isoelectronic organometallic iridium(III) complexes, *Inorg. Chem.* 50 (2011) 5777–5783.
- [57] K. Strohfeldt, M. Tacke, Bioorganometallic fulvene-derived titanocene anti-cancer drugs, *Chem. Soc. Rev.* 37 (2008) 1174–1187.
- [58] A. Kyzioł, A. Gierniak, J. Gubernator, A. Markowski, M. Jeżowska-Bojczuk, U.K. Komarnicka, Copper(I) complexes with phosphine derived from sparfloxacin. Part III: multifaceted cell death and preliminary study of liposomal formulation of selected copper(I) complexes, *Dalton Trans.* 47 (2018) 1981–1992.
- [59] J. Lopes, D. Alves, T.S. Morais, P.J. Costa, M.F.M. Piedade, F. Marques, M.J. Villa de Brito, M.H. Garcia, New copper(I) and heteronuclear copper(I)–ruthenium(II) complexes: synthesis, structural characterization and cytotoxicity, *J. Inorg. Biochem.* 169 (2017) 68–78.
- [60] S. Sperandio, K. Poksay, I. de Belle, M.J. Lafuente, B. Liu, J. Nasir, D.E. Bredesen, Paraptosis: mediation by MAP kinases and inhibition by AIP-1/Alix, *Cell Death Differ.* 11 (2004) 1066–1075.
- [61] A. Barilli, C. Atzeri, I. Bassanetti, F. Ingolia, V. Dall'Asta, O. Bussolati, M. Maffini, C. Mucchino, L. Marchiò, Oxidative stress induced by copper and iron complexes with 8-hydroxyquinoline derivatives causes paraptotic death of HeLa cancer cells, *Mol. Pharm.* 11 (2014) 1151–1163.
- [62] V. Gandin, M. Porchia, F. Tisato, A. Zanella, E. Severin, A. Dolmella, C. Marzano, Novel mixed-ligand copper(I) complexes: role of diimine ligands on cytotoxicity and genotoxicity, *J. Med. Chem.* 56 (2013) 7416–7430.
- [63] M. Porchia, F. Tisato, M. Zancato, V. Gandin, C. Marzano, In vitro antitumor activity of water-soluble copper(I) complexes with diimine and monodentate phosphine ligands, *Arab. J. Chem.* (2017), <http://dx.doi.org/10.1016/j.arabjc.2017.09.003>.
- [64] N. González-Ballesteros, D. Pérez-Álvarez, M. Carmen Rodríguez-Argüelles, M.S.C. Henriques, J.A. Paixão, S. Prado-López, Synthesis, spectral characterization and X-ray crystallographic study of new copper(I) complexes. Antitumor activity in colon cancer, *Polyhedron* 119 (2016) 112–119.
- [65] A. Bykowska, U.K. Komarnicka, M. Jeżowska-Bojczuk, A. Kyzioł, CuI and CuII complexes with phosphine derivatives of fluoroquinolone antibiotics – a comparative study on the cytotoxic mode of action, *J. Inorg. Biochem.* 181 (2018) 1–10.
- [66] Y. Wanga, X. Zhub, Z. Yanga, X. Zhaoa, Honokiol induces caspase-independent paraptosis via reactive oxygen species production that is accompanied by apoptosis in leukemia cells, *Biochem. Biophys. Res. Commun.* 430 (2013) 876–882.
- [67] S. Sperandio, I. de Belle, D.E. Bredesen, An alternative, nonapoptotic form of programmed cell death, *Proc. Natl. Acad. Sci. U. S. A.* 97 (2000) 14376–14381.
- [68] W.B. Wang, L.X. Feng, Q.X. Yue, W.Y. Wu, S.H. Guan, B.H. Jiang, M. Yang, X. Liu, D.A. Guo, Paraptosis accompanied by autophagy and apoptosis was induced by celastrol, a natural compound with influence on proteasome, ER stress and Hsp90, *J. Cell. Physiol.* 227 (2011) 2196–2206.
- [69] S. Elmore, Apoptosis: a review of programmed cell death, *Toxicol. Pathol.* 35 (2007) 495–516.
- [70] M.R.A.V. Ng, P.J. Antonelli, J. Joseph, Assessment of mitochondrial membrane potential in HEI-OC1 and LLC-PK1 cells treated with gentamicin and mitoquinone, *Otolaryngol. Head Neck Surg.* 152 (2015) 729–733.
- [71] H. Tarek, R. Mahmoud, M. Parviz, A. Charles, A. Kuszynski, E. Thomas, Natural retinoids inhibit proliferation and induce apoptosis in pancreatic cancer cells previously reported to be retinoid resistant, *Cancer Biol. Ther.* 4 (2005) 480–489.
- [72] S. Kalghatgi, C.S. Spina, J.C. Costello, M. Liesa, J.R. Morones-Ramirez, S. Slomovic, A. Molina, O.S. Shirihai, J.J. Collins, Bactericidal antibiotics induce mitochondrial dysfunction and oxidative damage in mammalian cells, *Antibiotics* 5 (2013) 192–285.
- [73] Y. Shi, Caspase activation, inhibition, and reactivation: a mechanistic view, *Protein Sci.* 13 (2004) 1979–1987.
- [74] Y.E. Henrotin, P. Bruckner, J.P. Pujol, The role of reactive oxygen species in homeostasis and degradation of cartilage, *Osteoarthr. Cartil.* 11 (2003) 747–755.
- [75] N. Fozia, A. Wustholz, R. Kinscherf, N.A. Metzler-Nolte, A cobaltocenium–peptide bioconjugate shows enhanced cellular uptake and directed nuclear delivery, *Angew. Chem. Int. Ed.* 44 (2005) 2429–2432.
- [76] S.M. Bianchi, L.R. Prince, K. McPhillips, L. Allen, H.M. Marriott, G.W. Taylor, P.G. Hellewell, I. Sabroe, D.H. Dockrell, P.W. Henson, M.K. Whyte, Impairment of apoptotic cell engulfment by pyocyanin, a toxic metabolite of *Pseudomonas aeruginosa*, *Am. J. Respir. Crit. Care Med.* 177 (2008) 35–43.